

สเทียเรต-ไกลเลต-เอ็น-ไตรเมทิลโคโคซานไมเซลล์ที่มีสมบัติยึดติดเยื่อเมือกสำหรับตัวนำส่ง
ยาซิมาวาสแตติน



นายจักรี นันทวิริยานนท์

จุฬาลงกรณ์มหาวิทยาลัย

CHULALONGKORN UNIVERSITY

บทคัดย่อและแฟ้มข้อมูลฉบับเต็มของวิทยานิพนธ์ตั้งแต่ปีการศึกษา 2554 ที่ให้บริการในคลังปัญญาจุฬาฯ (CUIR)
เป็นแฟ้มข้อมูลของนิสิตเจ้าของวิทยานิพนธ์ ที่ส่งผ่านทางบัณฑิตวิทยาลัย

The abstract and full text of theses from the academic year 2011 in Chulalongkorn University Intellectual Repository (CUIR)
are the thesis authors' files submitted through the University Graduate School.

วิทยานิพนธ์นี้เป็นส่วนหนึ่งของการศึกษาตามหลักสูตรปริญญาวิทยาศาสตรมหาบัณฑิต

สาขาวิชาปิโตรเคมีและวิทยาศาสตร์พอลิเมอร์

คณะวิทยาศาสตร์ จุฬาลงกรณ์มหาวิทยาลัย

ปีการศึกษา 2557

ลิขสิทธิ์ของจุฬาลงกรณ์มหาวิทยาลัย

MUCOADHESIVE STEARATE-GALLATE-N-
TRIMETHYLCHITOSAN MICELLES FOR SIMVASTATIN DELIVERY
CARRIERS

Mr. Jakkri Nunthaviriyant



A Thesis Submitted in Partial Fulfillment of the Requirements
for the Degree of Master of Science Program in Petrochemistry and Polymer Science
Faculty of Science
Chulalongkorn University
Academic Year 2014
Copyright of Chulalongkorn University

Thesis Title	MUCOADHESIVE STEARATE-GALLATE-N- TRIMETHYLCHITOSAN MICELLES FOR SIMVASTATIN DELIVERY CARRIERS
By	Mr. Jakkri Nunthaviriyant
Field of Study	Petrochemistry and Polymer Science
Thesis Advisor	Associate Professor Nongnuj Muangsin, Ph.D.

Accepted by the Faculty of Science, Chulalongkorn University in Partial
Fulfillment of the Requirements for the Master's Degree

.....Dean of the Faculty of Science
(Professor Supot Hannongbua, Dr.rer.nat.)

THESIS COMMITTEE

.....Chairman
(Assistant Professor Warinthorn Chavasiri, Ph.D.)

.....Thesis Advisor
(Associate Professor Nongnuj Muangsin, Ph.D.)

.....Examiner
(Assistant Professor Supaporn Noppakundilokrat, Ph.D.)

.....External Examiner
(Assistant Professor Nalena Praphairaksit, Ph.D.)

จักรี นันทวิริยานนท์ : สเตียรอยด์-แกลเลต-เอ็น-ไตรเมทิลโคโทซานไมเซลล์ที่มีสมบัติยึดติดเยื่อเมือกสำหรับตัวนำส่งยาซิมวาสแตติน (MUCOADHESIVE STEARATE-GALLATE-N-TRIMETHYLCHITOSAN MICELLES FOR SIMVASTATIN DELIVERY CARRIERS) อ.ที่ปรึกษาวิทยานิพนธ์หลัก: รศ. ดร.นงนุช เหมืองสิน, 113 หน้า.

วัตถุประสงค์ของการศึกษานี้คือการสังเคราะห์สเตียรอยด์-แกลเลต-เอ็น-ไตรเมทิลโคโทซานไมเซลล์ที่มีสมบัติยึดติดเยื่อเมือกให้มีสมบัติเหมาะสมสำหรับการนำส่งซิมวาสแตติน ซึ่งทำได้สำเร็จโดยการดัดแปรโคโทซานด้วยกรดกลูติก (GA) และกรดสเทียริก (SA) คอนจูเกตกับไตรเมทิลโคโทซาน โดยใช้ 1-ethyl-3-(3-dimethylaminopropyl)carbodiimide (EDAc) เป็น coupling agent ผลการศึกษาชี้ให้เห็นว่าดีกรีควอเตอร์ไนซ์เซชันของ TMC คือ 24.33 เปอร์เซ็นต์ การแทนที่ของ GA และ SA มีค่าประมาณ 5.00 และ 21.77 เปอร์เซ็นต์ ตามลำดับ คำนวณโดยเทคนิค $^1\text{H NMR}$ ค่าความเข้มข้นวิกฤตที่ทำให้เกิดไมเซลล์เท่ากับ 3.98 ไมโครกรัมต่อมิลลิลิตร ศึกษาความสามารถในการยึดติดเยื่อเมือกของพอลิเมอร์ที่ทดสอบด้วย Periodic acid: Schiff (PAS) ในของเหลวจำลองระบบทางเดินอาหาร (pH 1.2, 4.0 และ 6.4) ชี้ให้เห็นว่า SA-GA-TMC ให้ความสามารถในการยึดติดเยื่อเมือก 11.15, 5.82 และ 7.85 เท่า ที่ pH 1.2, 4.0 และ 6.4 ตามลำดับ เมื่อเทียบกับโคโทซานที่ไม่ได้ดัดแปร นอกจากนี้เมื่อทำการประยุกต์ใช้โคโทซานที่ดัดแปรเพื่อเป็นตัวนำส่งยาประเภทความสามารถละลายน้ำต่ำ โดยใช้ซิมวาสแตตินเป็นยาจำลอง ซึ่งมีประสิทธิภาพในการกักเก็บยามากกว่า 80 เปอร์เซ็นต์ ความสามารถยึดติดเยื่อเมือกของอนุภาค SV-SA-GA-TMC มีค่า 1.35, 1.51 และ 1.68 มิลลิกรัมต่อมิลลิลิตร ในสภาวะ pH 1.2, 4.0 และ 6.4 ตามลำดับ นอกจากนี้อนุภาคนี้นั้นยังสามารถปลดปล่อยซิมวาสแตตินนาน 24 ชั่วโมง

จุฬาลงกรณ์มหาวิทยาลัย
CHULALONGKORN UNIVERSITY

สาขาวิชา ปีโตรเคมีและวิทยาศาสตร์พอลิเมอร์ ลายมือชื่อนิสิต

ปีการศึกษา 2557 ลายมือชื่อ อ.ที่ปรึกษาหลัก

5571935323 : MAJOR PETROCHEMISTRY AND POLYMER SCIENCE

KEYWORDS: CHITOSAN/ MICELLE/ MUCOADHESIVE/ SIMVASTATIN

JAKKRI NUNTHAVIRIYANONT: MUCOADHESIVE STEARATE-GALLATE-*N*-TRIMETHYLCHITOSAN MICELLES FOR SIMVASTATIN DELIVERY CARRIERS. ADVISOR: ASSOC. PROF. NONGNUJ MUANGSIN, Ph.D., 113 pp.

This study aimed to prepare a mucoadhesive stearate-gallate-*n*-trimethylchitosan micelles for simvastatin delivery carriers. This can be achieved by modification of chitosan with gallic acid (GA) and stearic acid (SA) conjugated with *N*-trimethylchitosan using 1-ethyl-3-(3-dimethylaminopropyl)carbodiimide (EDAc) as a coupling agent. The results indicated that the degree of quaternization (DQ) of TMC was 24.33%. The substitution of GA and SA was about 5.00 and 21.77 % by ^1H NMR, respectively. Critical micelle concentration (CMC) was found that the SA-GA-TMC was 3.98 $\mu\text{g}/\text{mL}$. Periodic acid: Schiff (PAS) colorimetric method was used to study mucin conjugated polymer in the simulated gastrointestinal fluid (pH 1.2, 4.0 and 6.4). The SA-GA-TMC showed stronger mucoadhesive property 11.15, 5.82 and 7.85 times, respectively than that of unmodified chitosan at pH 1.2, 4.0 and 6.4, respectively. Additionally, the application of SA-GA-TMC as low water soluble drug delivery carriers was investigated using simvastatin (SV) as a model drug. The SV loaded micelles exhibited over 80% drug entrapment efficiency. The mucoadhesiveness of SV-SA-GA-TMC micelles displayed 1.35, 1.51 and 1.68 mg/mL at pH 1.2, 4.0 and 6.4, respectively. The release profiles of SV-SA-GA-TMC showed prolonged and sustained drug release over 24h.

CHULALONGKORN UNIVERSITY

Field of Study: Petrochemistry and Polymer Science Student's Signature

Science Advisor's Signature

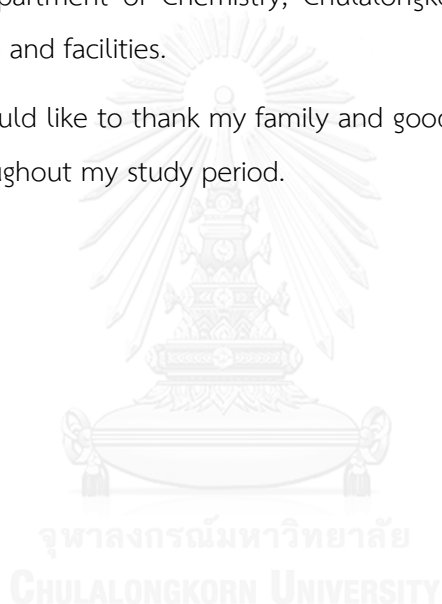
Academic Year: 2014

ACKNOWLEDGEMENTS

I would like to express my sincere gratitude to my advisor Associate Professor Dr. Nongnuj Muangsin for her valuable guidance and suggestions at Chulalongkorn University. I wish to thank my graduate committee members, Assistant Professor Dr. Warinthorn Chavasiri, Assistant Professor Dr. Supaporn Noppakundilograt and Assistant Professor Dr. Nalena Praphairaksit for their helpful advice comment.

Moreover, I would like to thank the Research Centre for Petrochemical and polymer science, Department of Chemistry, Chulalongkorn University for the use of equipment, glassware and facilities.

Finally, I would like to thank my family and good friends for their support and encouragement throughout my study period.



CONTENTS

	Page
THAI ABSTRACT	iv
ENGLISH ABSTRACT	v
ACKNOWLEDGEMENTS	vi
CONTENTS	vii
CHAPTER I INTRODUCTION.....	7
1.1 Introduction.....	7
1.2 The objectives of this research	17
1.3 The scope of research.....	17
CHAPTER II THEORY AND LITERATURE REVIEWS	22
2.1 Hypercholesterolemia	22
2.2 Simvastatin.....	23
2.2.1 Structure	23
2.2.2 Physical and chemical properties.....	24
2.3 Controlled release system	25
2.3.1 Controlled release mechanisms.....	29
2.4 Mucoadhesive system	30
2.4.1 Mechanisms of mucoadhesion	31
2.4.2 Mucoadhesion theories	32
2.4.2.1 Electronic Theory	33
2.4.2.2 Wetting Theory.....	33
2.4.2.3. Adsorption Theory.....	34
2.4.2.4. Diffusion Theory.....	34

	Page
2.4.2.5. Mechanical Theory.....	35
2.4.2.6. Cohesive Theory.....	35
2.4.3 The mucoadhesive/mucosa interaction.....	35
2.4.3.1. Physical interactions.....	35
2.4.3.2. chemical interactions.....	36
2.4.4 Mucoadhesive polymers.....	37
2.5 Technique to prepare micelles.....	38
2.5.1 Methods for preparation of nanoparticles from dispersion of preformed polymer.....	38
CHAPTER III EXPERIMENTAL.....	40
3.1 Materials.....	40
3.1.1 Model drug.....	40
3.1.2 Polymer.....	40
3.1.3 Chemicals.....	40
3.2 Instruments.....	41
3.3 Methods.....	42
3.3.1 Synthesis of Stearate-gallate- <i>N</i> -trimethylchitosan.....	42
3.3.1.1 Synthesis of <i>N</i> -trimethylchitosan (TMC).....	42
3.3.1.2 Synthesis of GA-TMC conjugate.....	42
3.3.1.3 Synthesis of SA-GA-TMC conjugate.....	43
3.3.2 Chemical characterization.....	44
3.3.2.1 Fourier transformed infrared spectroscopy (FT-IR).....	44
3.3.2.2 ¹ H Nuclear Magnetic Resonance spectroscopy (¹ H NMR).....	45

	Page
3.3.2.3 Critical Micelle Concentration (CMC) determination.....	46
3.3.3 In vitro bioadhesion of mucin to chitosan and modified chitosan	46
3.4 Pharmaceutical applications.....	48
3.4.1 Preparation of drugs-loaded SA-GA-TMC micelles.....	48
3.4.2 Characterization of the SA-GA-TMC micelles	49
3.4.2.1 Scanning Electron Microscope (SEM).....	49
3.4.2.2 Particle size measurement	49
3.4.2.3 Zeta potential	50
3.4.2.4 Fourier Transform Infrared (FTIR) Spectroscopy.....	50
3.4.3 Study of the drug behavior of the micelles.....	50
3.4.3.1 Calibration curve of SV.....	50
3.4.3.2 Calibration curve of SV in pH 1.2, 4.0 and 6.4.....	51
3.4.3.3 Determination of encapsulation and drug loading efficiency (%EE).....	51
3.4.3.4 In vitro drug release.....	52
3.4.4 Statistical analysis	53
CHAPTER IV RESULTS AND DISCUSSION	54
4.1 Synthesis of TMC, GA-TMC AND SA-GA-TMC.....	54
4.2.1 Fourier transformed infrared spectroscopy (FT-IR)	55
4.2.2 ¹ H Nuclear Magnetic Resonance spectroscopy (¹ H NMR).....	57
4.3 Self-Assembly Morphologies.....	60
4.3.1 Effects of speed and time on self-assembly	60
4.3.2 Effects of concentrations on self-assembly	62

	Page
4.3.3 Critical Micelle Concentration (CMC) determination	65
4.4 Mucoadhesive properties	66
4.4.1 Assessment of the mucoadhesive behavior of CS, TMC, GA-TMC and SA-GA-TMC by mucus glycoprotein assay	66
4.4.2 Adsorption of mucin on polymer.....	67
4.5 Morphology of SA-GA-TMC with SV encapsulation	70
4.5.1 Particles size, size distribution.....	72
4.5.2 Zeta potential (Zp).....	72
4.5.3 Mucoadhesiveness of SA-GA-TMC with SV	75
4.6 Characterization of SA-GA-TMC micelle with SV.....	76
4.6.1 Fourier transform infrared spectroscopy (FTIR)	76
4.7 Evaluation of drug encapsulation and drug loading efficiency (%EE and % DL).....	78
4.8 In vitro release profiles	79
CHAPTER V CONCLUSION AND SUGGESTION	84
5.1 Conclusion	84
5.2 Suggest.....	85
REFERENCES	86
APPENDIX A Calibration curve of mucin (type II).....	96
APPENDIX B Calibration curve of SV.....	101
APPENDIX C Encapsulation and Cumulative Drug Release	106
Appendix D Particle size of micelles	111
VITA.....	113

LIST OF TABLE

Table		Page
1.1	Chitosan-based polymeric micelles for low water soluble drug peroral delivery.....	15
3.1	The Instruments used in this study.....	41
4.1	SEM images of prepared self-assemblies with various speed and time by vortexing of SA-GA-TMC concentration 1 mg/mL.....	62
4.2	Comparison of chitosan and modified chitosan (TMC, GA-TMC and SA-GA-TMC) to mucoadhesive property.....	68
4.3	Properties of Synthesized chitosan micelles and Prepared SV Loaded SA-GA-TMC micelles.....	74
4.4	Encapsulation and drug loading of SV loaded SA-GA-TMC.....	79

LIST OF FIGURE

Figure	Page
1.1 Chemical structure of simvastatin.....	8
1.2 Chemical structure of chitosan.....	11
1.3 Structure of <i>N</i> -trimethyl chitosan (TMC).....	11
1.4 Synthesis scheme of stearate-gallate- <i>N</i> -trimethyl chitosan (SA-GA-TMC).....	14
1.5 Description of the structural micelle by dialysis method.....	16
1.6 Scheme of SV loaded mucoadhesive polymeric micelle.....	17
2.1 A continued build of fatty (atheroma) within artery walls.....	22
2.2 Chemical structure of Simvastatin in lactone and hydroxyl acid forms.....	24
2.3 Pathway of simvastatin inhibit the conversion of 3-hydroxy-3-methylglutaryl coenzyme A (HMG-CoA) to l-mevalonate, the rate-limiting step of the cholesterol synthesis pathway.....	25
2.4 Drug concentrations at site of therapeutic action after delivery as a conventional injection (thin line) and as a temporal controlled release system.....	27
2.5 Representation of controlled release drug system.....	28
2.6 Drug delivery from carrier system.....	29

Figure	Page
2.7 Mechanism of mucoadhesion.....	31
2.8 The two stages of the mucoadhesion process.....	32
2.9 Schematic diagram showing influence of contact angle between device and mucous membrane on bioadhesion.....	33
2.10 Secondary interactions resulting from interdiffusion of polymer chains of bioadhesive device and of mucus.....	34
2.11 Schematic representation of dialysis method for preparation of polymeric micelles.....	39
3.1 Synthesis flowchart of Stearate-gallate- <i>N</i> -trimethylchitosan (SA- GA-TMC).....	44
4.1 Synthesis flowchart of stearate-gallate- <i>N</i> -trimethyl chitosan (SA- GA-TMC).....	54
4.2 FTIR spectra of CS (a), TMC (b), GA (c), GA-TMC (d) and SA-GA- TMC (e).....	56
4.3 Representative ¹ HNMR spectra of (a) CS, (b) TMC, (c) GA, (d) GA- TMC and (e) SA-GA-TMC.....	59

Figure	Page
4.4 SEM images of self-assemblies with various SA-GA-TMC concentrations: a) 0.2, b) 0.4, c) 0.6, d) 0.8 e) 1.0 and f) 1.4 mg/mL at 2h and 2400 rpm for 2 d.....	64
4.5 EDX spectrum of cubic self-assemblies of SA-GA-TMC (1mg/mL) suggested it is rich in both C and O.....	64
4.6 Plot of intensity ratio I_{374}/I_{384} as polymer concentrations.....	65
4.7 Adsorption of mucin on CS, TMC, GA-TMC and SA-GA-TMC at pH 1.2, 4.0 and 6.4. Data are shown as the mean \pm SD and derived from three independent repeats.....	70
4.8 Representative SEM images of SA-GA-TM (1a-b) with 10% SV and SA-GA-TMC (2a-b) with 20% SV.....	71
4.9 Adsorption of mucin on SA-GA-TMC micelles with SV at pH 1.2, 4.0 and 6.4. Data are shown as the mean \pm SD.....	75
4.10 FTIR spectra of (a) SV, (b) 10% SV-SA-GA-TMC and (c) 20% SV-SA-GA-TMC micelles.....	77
4.11 Release profiles of 10% simvastatin from SA-GA-TMC micelles in three different buffers, $37 \pm 1^\circ\text{C}$ (average \pm SD, n=3).....	80

Figure		Figure
4.12	Release profiles of 10% and 20% simvastatin from SA-GA-TMC micelles in pH 1.2 buffers, 37 ± 1 °C (average \pm SD, n=3).....	81
4.13	Release profiles of 10% and 20% simvastatin from SA-GA-TMC micelles in pH 4.0 buffers, 37 ± 1 °C (average \pm SD, n=3).....	82
4.14	Release profiles of 10% and 20% simvastatin from SA-GA-TMC micelles in pH 6.4 buffers, 37 ± 1 °C (average \pm SD, n=3).....	83



LIST OF ABBREVIATIONS

g	gram
μg	microgram
mg	milligram
mL	milliliter
nm	nanometer
μm	micrometer
h	hour
mL/h	milliliter per hour
cm	centimeter
kV	kilovolt
kDa	kilodalton
°C	degree Celsius (centigrade)
CS	chitosan
TMC	<i>N</i> -trimethylchitosan
GA	gallic acid
SA	stearic acid
SV	simvastatin
EDAC	1-Ethyl-3-(3-dimethylaminopropyl)carbodiimide
FTIR	Fourier Transform Infrared Spectrophotometer
SEM	Scanning Electron Microscope
%DD	degree of deacetylation
EE	entrapment efficiency
DL	drug loading efficiency
PDI	polydispersity index
MW	molecular weight
ppm	part per million
pH	power of hydrogen ion or the negative logarithm (base ten)
r ²	correlation coefficient
S.D.	standard deviation
rpm	round per minute

CHAPTER I

INTRODUCTION

1.1 Introduction

Simvastatin (SV) (Figure 1.1) is a commercial drug belongs to a group of 3-hydroxy-3-methylglutaryl-coenzyme A (HMG CoA) reductase inhibitors. It is widely used for treat of primary hypercholesterolemia and cardiovascular diseases [1]. After oral administration, an inactive lactone form of simvastatin is converted to an active form of β -hydroxyacid in liver. This is a potent competitive inhibitor and widely use of 3-hydroxyglutaryl-CoA reductase the enzyme, which is a catalyzes the rate-limiting step of cholesterol biosynthesis [2].

The disadvantage of simvastatin for oral administration is approximately insoluble in water with solubility of 30 $\mu\text{g/mL}$ [3], short biological half-life (3 h) and poorly absorbed in the gastrointestinal tract (GI) (<5%) [4]. Since 95% of orally administered SV is retained by the liver [5, 6], only 5% of the SV oral formulation is absorbed for gastrointestinal tract (GI). However, higher oral administration doses may increase the apportionment of SV to target but are impractical due to the associated systemic toxicities [5, 6]. Due to this are disadvantages of low water soluble drug such as simvastatin. Therefore, the polymeric micelle system is considered to be a promising technique for reducing the toxic side effects, enhancing the bioavailability and using the polymer carrier of simvastatin because the polymeric micelle showed

higher drug release profiles is suitable for sustaining and an amount of SV is increased release of SV than pure SV [7, 8]. Moreover, polymer carriers are capable of attaching to mucosal surfaces and polymer carriers are gradually release of drug. Therefore, it is practically necessary for the delivery of water-insoluble drugs to develop a material with better biocompatibility and sustained release. In recent years much attention has been focused on mucoadhesive SV, development mucoadhesive buccal tablets of SV using mucoadhesive polymers found that the polymer restrained the release of SV and the absorption of SV improved [9].

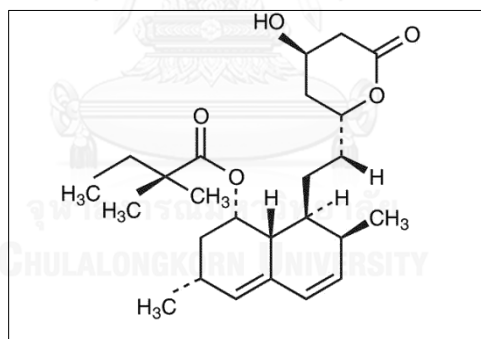


Figure 1.1 Chemical structure of simvastatin

The potential use for mucoadhesive systems as drug carriers lies in its prolongation of the residence time at the absorption site, allowing intensified contact with the epithelial barrier [10]. The mechanism of mucoadhesion is generally

distributed in two steps, the contact stage and the consolidation stage. The first stage is characterized by the contact between the mucoadhesive and the mucous membrane, with spreading and swelling of the formulation, initiating its deep contact with the mucus layer. The drugs that are absorbed through the mucosal lining of tissues can enter directly into the blood stream and not be inactivated by enzymatic degradation in the gastrointestinal tract and an increase in drug concentration gradient on the mucosa, as a result, the bio-availability of drug can be improved [11-13]. Due to these advantages, many attempts have been made to improve the mucoadhesive properties of polymeric carriers.

The design and selection of polymers for drug delivery is partially based on the concept that mucoadhesive polymers should have functional groups and active site, which can be summarized as follows:

- 1) Hydroxyl (-OH) and amide (-NH₂) groups, or strong anionic or positive charges
- 2) Carboxyl (-COOH) and hydroxyl (-OH), hydrogen-bonding group
- 3) High molecular weight
- 4) Sufficient chain flexibility

These polymers would be able to interact more strongly to the mucus glycolproteins [14, 15].

Chitosan (Figure 1.2) is a reasonable option for peroral drug delivery due to its biodegradability, biocompatibility, permeation enhancing effect, and mucoadhesion [16, 17]. Due to the properties of chitosan, micelles based on chitosan can protect low water soluble drugs from degradation in the GI tract and improve drug absorption. Chitosan itself has a certain antitumor activity and its positive charge can neutralize the negative charge on the tumor cell surface, resulting in selective absorption [18]. Moreover, since chitosan is a hydrophilic and cationic polysaccharide with high chemical reactivity, chitosan can be readily obtained by chemically attaching hydrophilic and hydrophobic parts to the backbone of chitosan [19]. Thus far, some chitosan-based micellar systems for peroral drug delivery have been developed and modifications of chitosan are designed for different purposes. Chitosan is soluble in dilute acidic solutions below pH 6.0 due to the quaternization of the amine groups that have a pKa value of 6.3 making chitosan promotes solubility, whereas chitosan is insoluble at alkaline and neutral pH. The primary amino group accounts for the possibility of relatively easy chemical modification of chitosan and salt formation with acids.

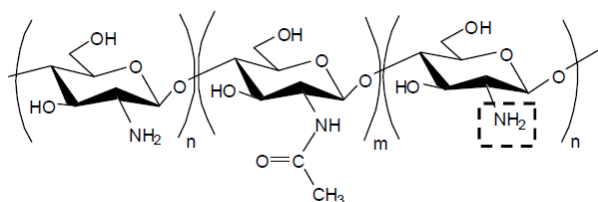


Figure 1.2 Chemical structure of chitosan

In last decade *N*-trimethyl chitosan (TMC) has appeared as one of the most promising mucoadhesive polymer that has greatly attracted the absorption enhancement effect of this polymer. TMC (Figure 1.3), a chemically modified derivative of chitosan and is shown to be the absorption enhancer for drugs across mucosal epithelia [20]. TMC shows good water solubility at a wide range of pH. The charge density of TMC was determined by the degree of quaternization, plays an important part in the absorption enhancing properties [21-23]. Mucoadhesive properties of TMC are explained by the formation of electrostatic interaction between positive charges of the TMC and negative charges sialic groups of the mucus [24].

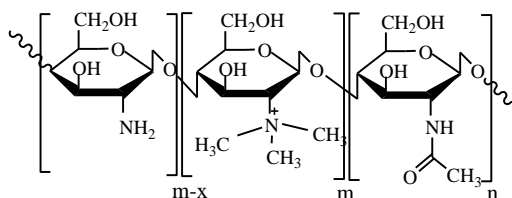


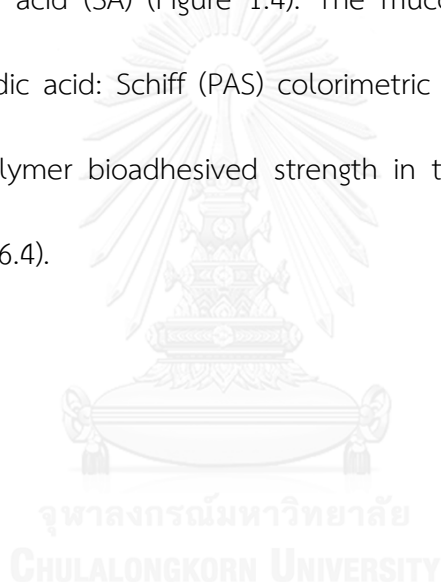
Figure 1.3 Structure of *N*-trimethyl chitosan (TMC)

In several recently studies, the self-assembly of amphiphilic polymeric micelles has been synthesized as promising micellar carriers for the low water soluble drug delivery. In previous studies, such as tocopherol succinate-chitosan micelles [25], *N*-deoxycholic acid-chitosan micelles [26], octyl-chitosan micelles [27] and stearic acid-chitosan micelles [28] are improved in comparison to the native chitosan. In general, amphiphilic polymers with hydrophilicity have compatibility with water molecules and lead to form self-assembled micelles, it can also still encapsulate hydrophobic drugs.

The recently reported, Zhenshan et al. [29] described the controlled release of Simvastatin (SV) from polymeric micelles *in vitro*. Xiangning et al. [30] constructed poly caprolactone (PCL) containing simvastatin concluded that the SV loaded PCL micelles may be used clinically in the near future for bone loss diseases, including osteoporosis. However, stearic acid-chitosan is kind of hydrophobic modification. The stearic acid-chitosan could form micelles in the aqueous solution. Furthermore, stearic acid-chitosan has the characterization of good solubility in distilled water, narrow size distribution, reduces cell toxicity and suitable positive charge [31] because it has significant benefits in terms of drug loading, release, delivery, and stability.

The aim of this study was to design and synthesize mucoadhesive chitosan micelles for delivery of simvastatin (as a model low water soluble drug). These mucoadhesive chitosan micelles designed in order to increase mucoadhesion and

obtain sustained release of the simvastatin from this polymeric micelles. This can be performed by (i) increase the positive charge of the modified chitosan, (ii) coupling an gallic acid (aromatic system) into the chitosan backbone to increase the hydrophobic molecules and to increase mucoadhesion property and finally, (iii) conjugate the stearic acid to increase hydrophobicity to form self-assembly micelles. This can be achieved by modification of chitosan to N-trimethyl chitosan with gallic acid (GA) and stearic acid (SA) (Figure 1.4). The mucoadhesive measurement was determined by Periodic acid: Schiff (PAS) colorimetric method was used to qualify mucin-conjugated polymer bioadhesives strength in the simulated gastrointestinal fluid (pH 1.2, 4.0 and 6.4).



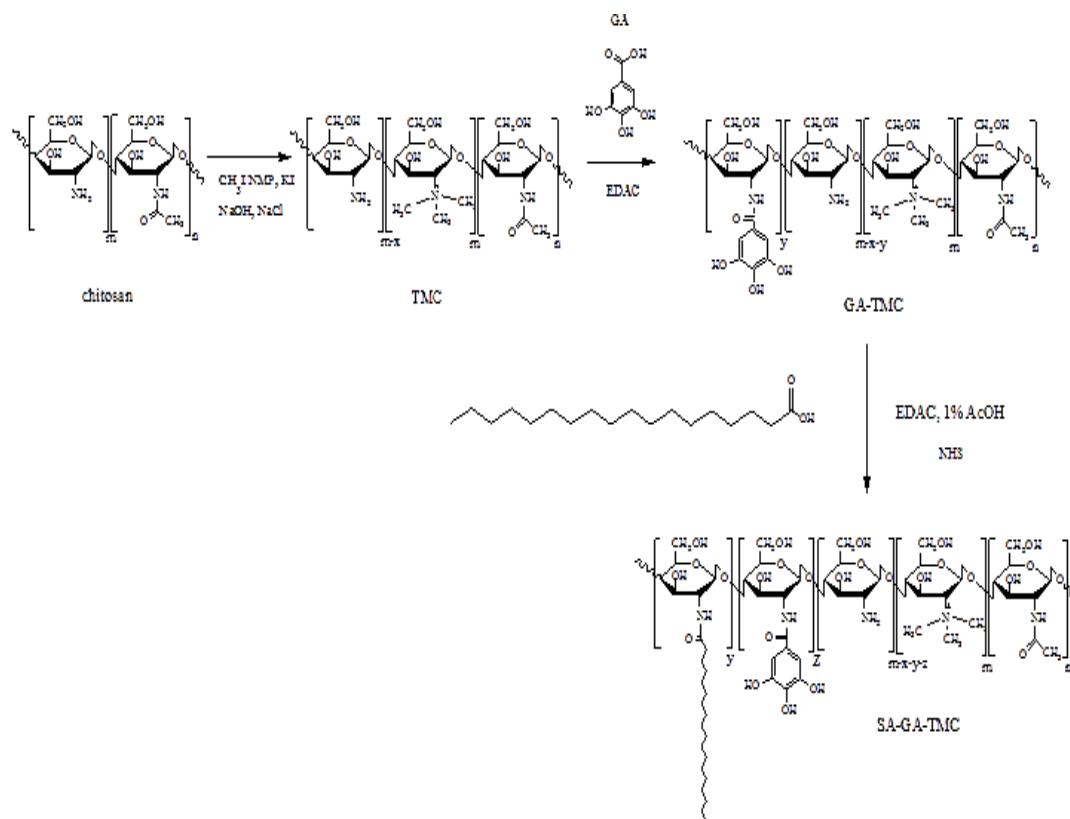


Figure 1.4 Synthesis scheme of stearate-gallate-*N*-trimethyl chitosan (SA-GA-TMC)

Several methods have been used to prepare chitosan-based polymeric micelles for drug peroral delivery system such as solvent evaporation method, chemical conjugation and dialysis method are summarized in Table 1.1. As the dialysis method (Figure 1.5) consists of supplanting a water-miscible solvent in which the low water soluble drug and copolymer are both soluble with a solvent that is selective only for the hydrophilic part of the polymer. As the good solvent is replaced by the selective one, the hydrophobic portion of the polymer associates to form the micellar core incorporating the insoluble drug in the process. Extending the

dialysis over several days helps ensure the complete removal of the organic solvent.

The advantage of dialysis method is containing amount of low water soluble drug in the hydrophobic core great than other methods [32].

Table 1.1 Chitosan-based polymeric micelles for low water soluble drug peroral delivery.

Material	Model drug	Modification purpose	Prepare method
Stearic acid - chitosan	Doxorubicin	Prolonging drug release	Dialysis
Chitosan	Docetaxel	Increasing solubility of insoluble drug	Chemical conjugation
Chitosan-tocopherol succinate	Itraconazole	Increasing the solubility of insoluble drug	Solvent evaporation method

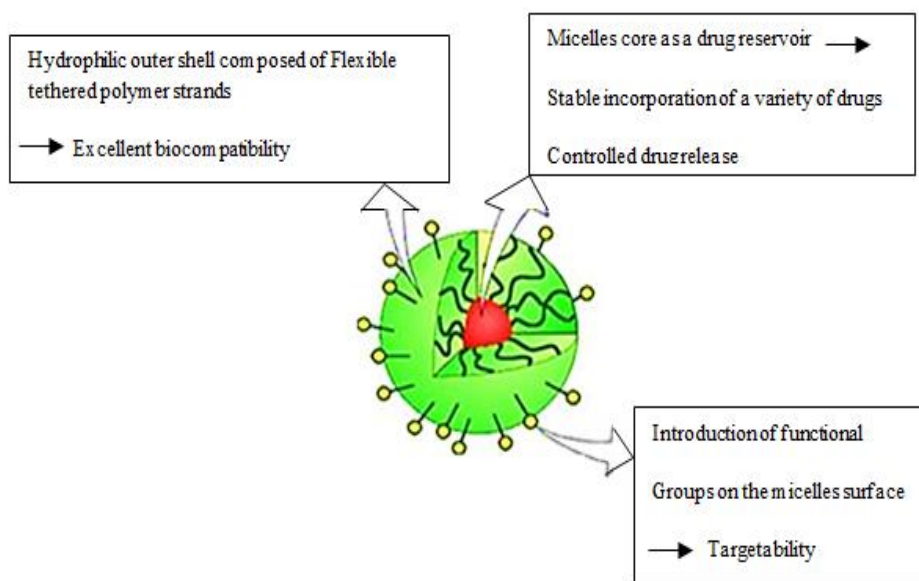


Figure 1.5 Description of the structural micelle by dialysis method [32]

Therefore, the present work was to prepare controlled release polymeric micelles of SV, using SA-GA-TMC as the retarding carrier by dialysis method (Figure 1.6) and study the in vitro release profiles of SV loaded SA-GA-TMC micelles in simulated gastrointestinal fluid pH 1.2, 4.0 and 6.4.

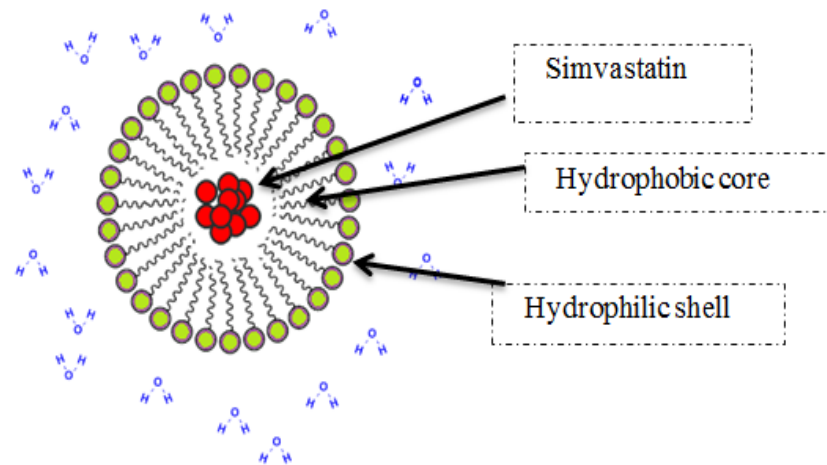


Figure 1.6 Scheme of SV loaded mucoadhesive polymeric micelle

1.2 The objectives of this research

- 1) Synthesize stearate-gallate-*N*-trimethyl chitosan micelle to improve mucoadhesive properties for delivery carriers.
- 2) Preparation of mucoadhesive stearate-gallate-*N*-trimethyl chitosan micelle for low water soluble drugs delivery.

1.3 The scope of research

The scope of this research was carried out by stepwise methodology as follows:

- 1) Review literature for related research work.
- 2) Part I: Synthetic stearate-gallate-*N*-trimethyl chitosan micelle
 - a. Preparation of *N*-trimethyl chitosan, gallate- *N*-trimethyl chitosan and stearate-gallate-*N*-trimethyl chitosan (TMC, GA-TMC and SA-GA-TMC)

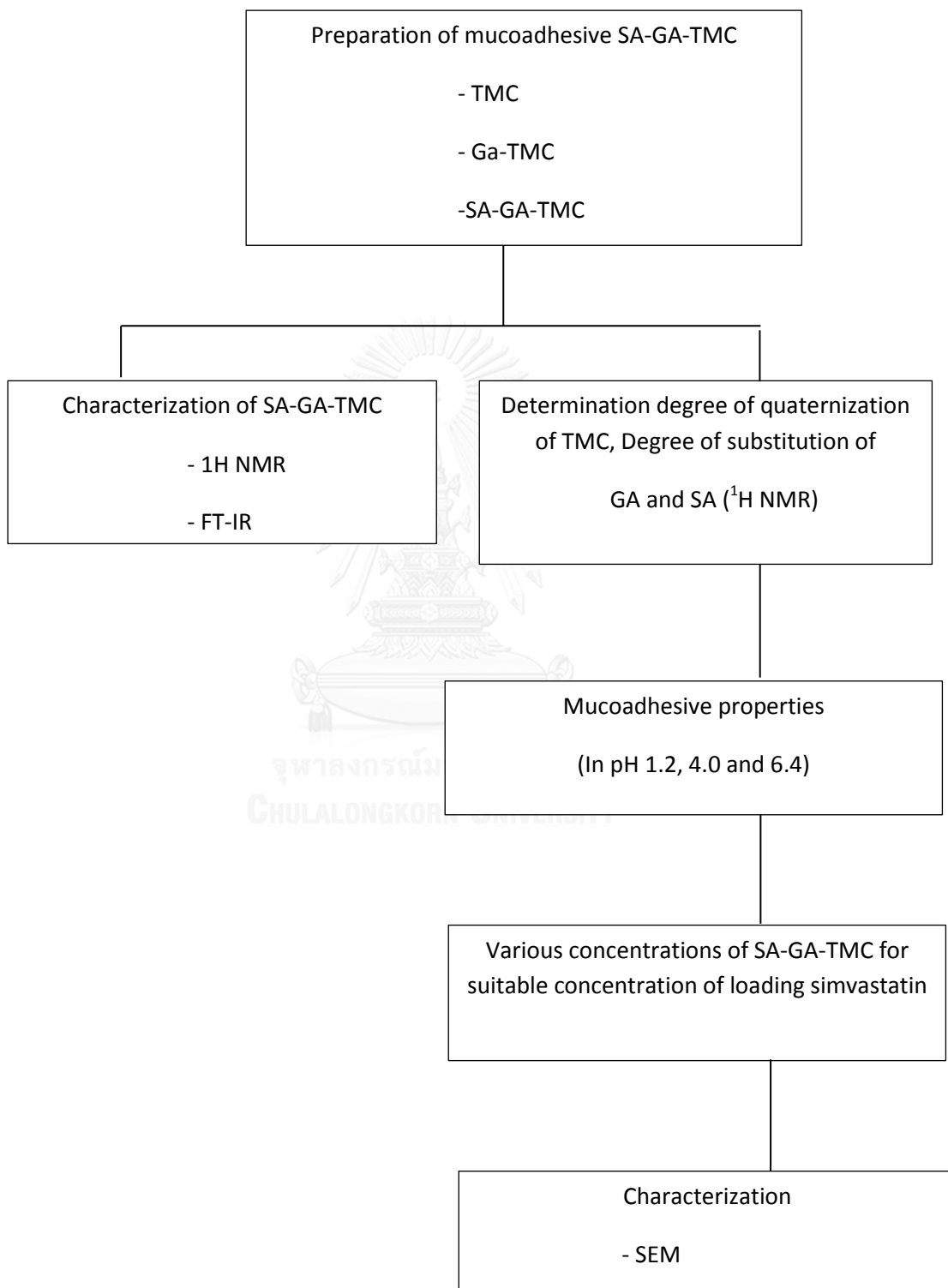
- b. Characterization of the physical and chemical properties of chitosan and modified chitosan using FTIR and $^1\text{H-NMR}$.
- c. Determination degree of quaternization of TMC.
- d. Determination degree of GA and SA substitution.
- e. In vitro investigation of mucoadhesive property in simulated gastrointestinal fluid (SGF) pH 1.2, 4.0 and the simulated intestinal fluid (SIF) pH 6.4 by using UV-Vis method.
- f. Preparation of particle size of the SA-GA-TMC with various concentrations of SA-GA-TMC for suitable concentration of loading simvastatin.
- g. Characterization of the obtained SA-GA-TMC micelles in terms of morphology, size by SEM.

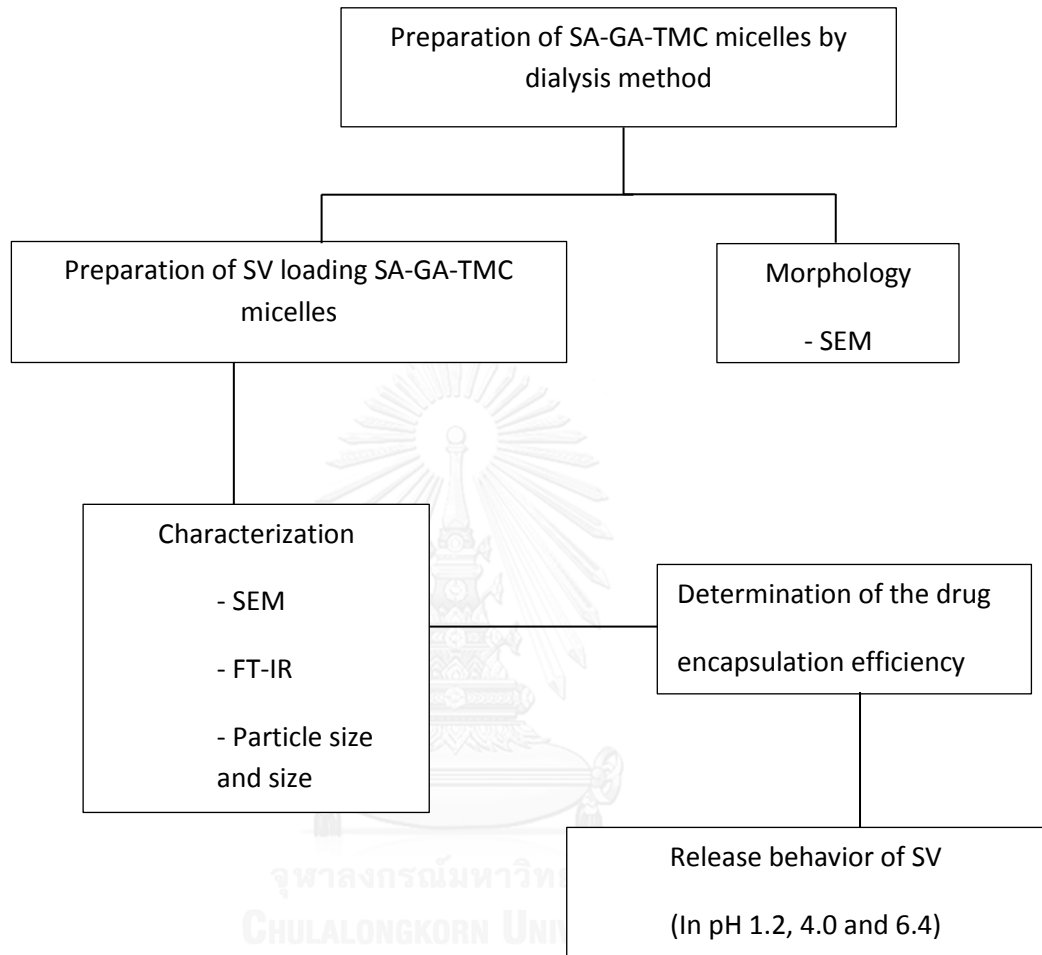
Part II: Fabrication and evaluation of the modified chitosan as a drug delivery carries.

- a. Preparation of the SA-GA-TMC micelles with and without drug
- b. Characterization of the obtained SA-GA-TMC micelles in term of morphology, size, size distribution, zeta potential and chemical analysis.
- c. Determination of the simvastatin encapsulation efficiency.

- d. In vitro investigation of mucoadhesive property in simulated gastrointestinal fluid (SGF) pH 1.2, 4.0 and the simulated intestinal fluid (SIF) pH 6.4 by using UV-Vis method.
 - e. Study the In vitro release behavior of the spheres in simulated gastrointestinal fluid pH 1.2, 4.0 and 6.4 using UV-Vis method.
- 3) Report, Discussion and Writing up thesis.



Part I: Flow chart for synthesis and characteristic

Part II: Pharmaceutical application

CHAPTER II

THEORY AND LITERATURE REVIEWS

2.1 Hypercholesterolemia

Hypercholesterolemia is the presence of high levels of fat or cholesterol in the blood. Cholesterol is a natural component of total the cell in the body. The level of cholesterol is higher than 240 mg is regarded as high. People with high cholesterol levels raise their risk for coronary artery disease. This hypercholesterolemia was occurred when excess cholesterol in the bloodstream is deposited in the walls of blood vessels (Figure 2.1) particularly in the arteries that supply blood to the heart. Simple actions including exercise and diet can help prevent hypercholesterolemia.

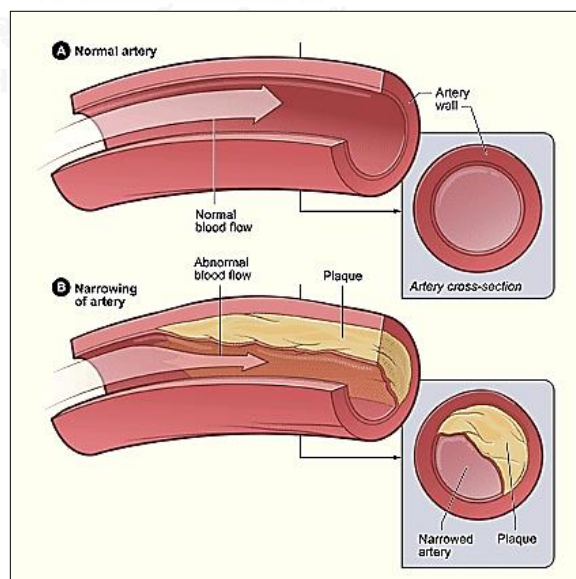


Figure 2.1 A continued build of fatty (atheroma) within artery walls

2.2 Simvastatin

Simvastatin (SV) is a synthetic derivation of a fermentation product of *Aspergillus terreus*, and marketed under the trade name of Zocor. It is a member of the statin that widely used for lowering cholesterol and other lipids (fats) in the blood to reduce the risk of heart disease problems but practically insoluble in water, short biological half-life, high first-pass metabolism and poorly absorbed from the gastrointestinal tract (GI).

2.2.1 Structure

Simvastatin is a nonhygroscopic white crystalline powder, insoluble in water but quite soluble in chloroform, methanol and alcohol with pKa of 4.68 [2]. The molecular weight of this compound $C_{25}H_{38}O_5$ is 418.57. Simvastatin is the pharmacologically inactive lactone form of simvastatin acid, butanoic acid, 2,2-dimethyl-1,2,3,7,8,8a-hexahydro-3,7-dimethyl-8-[2-(tetrahydro-4-hydroxy-6-oxo-2H-pyran-2-yl) ethyl]-1-naphthalenylbester. Simvastatin is a lactone which needs the opening of the ring for it to become active. Figure 2.2 shows the chemical structure of simvastatin [2, 33].

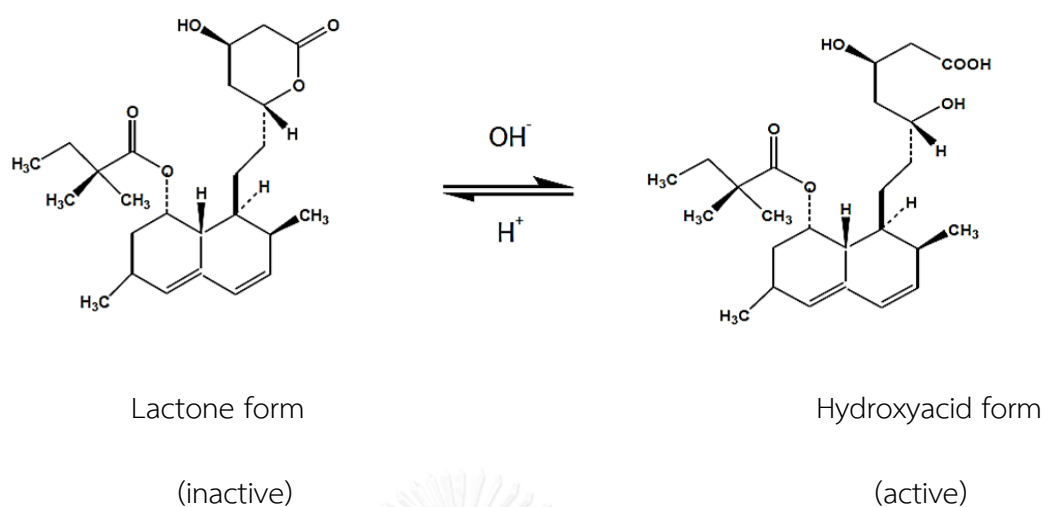


Figure 2.2 Chemical structure of Simvastatin in lactone and hydroxyl acid forms

2.2.2 Physical and chemical properties

Simvastatin in a lactone form (Figure 2.2) undergoes hydrolysis and is converted to its β , δ -dihydroxy acid form (simvastatin acid) by the cytochrome-3A system in liver, where it is a potent competitive inhibitor of 3-hydroxyglutaryl-CoA reductase the enzyme that catalyzes the rate-limiting step of cholesterol biosynthesis. This leads to up-regulation of low-density lipoprotein (LDL) receptors and an increase in catabolism of LDL cholesterol shown in figure 2.3.

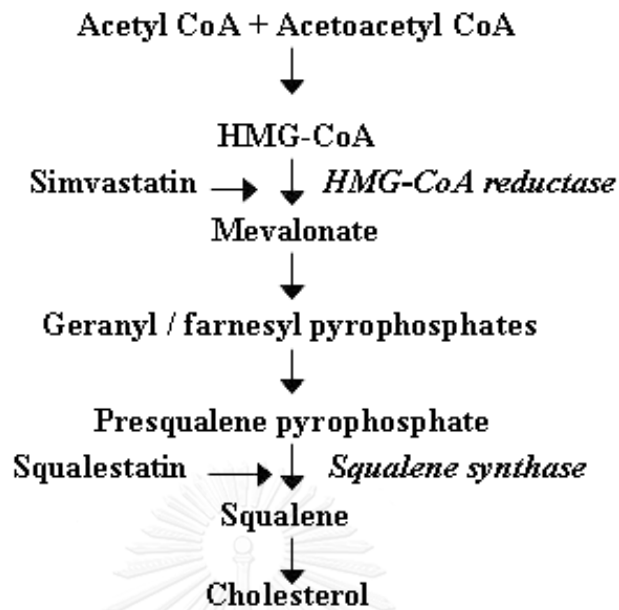


Figure 2.3 Pathway of simvastatin inhibit the conversion of 3-hydroxy-3-methylglutaryl coenzyme A (HMG-CoA) to l-mevalonate, the rate-limiting step of the cholesterol synthesis pathway

2.3 Controlled release system

In the past decade, controlled release drug systems from polymeric control are designed to enhance drug therapy. Many researchers are developing controlled release drug, which may attend to drug of interest. Controlled drug release system have been sustained delivery to enable over days/weeks/months or years and targeted delivery on one-time or sustained basis. Controlled release was designed to

prevent drug from premature eradicate from metabolism system within body, and to reduce the amount of drug necessary to cause the same therapeutic effect in patients.

Controlled release over an extended duration is highly beneficial for drugs that are rapidly metabolized and eliminated from the body after administration [34]. Controlled release over an extended duration is highly beneficial for drugs that are rapidly metabolized and eliminated from the body after administration [34]. An example of this benefit is shown schematically in Figure 2.4 in which the concentration of drug at the site of activity within the body is compared after immediate release from 4 injections administered at 6 hourly intervals and after extended release from a controlled release system. Drug concentrations may fluctuate widely during the 24 h period when the drug is administered via bolus injection, and for only a portion of the treatment period is the drug concentration in the therapeutic window (i.e., the drug concentration that produces beneficial effects without harmful side effects). With the controlled release system, the rate of drug release matches the rate of drug elimination and, therefore, the drug concentration is within the therapeutic window for the vast majority of the 24 h period.

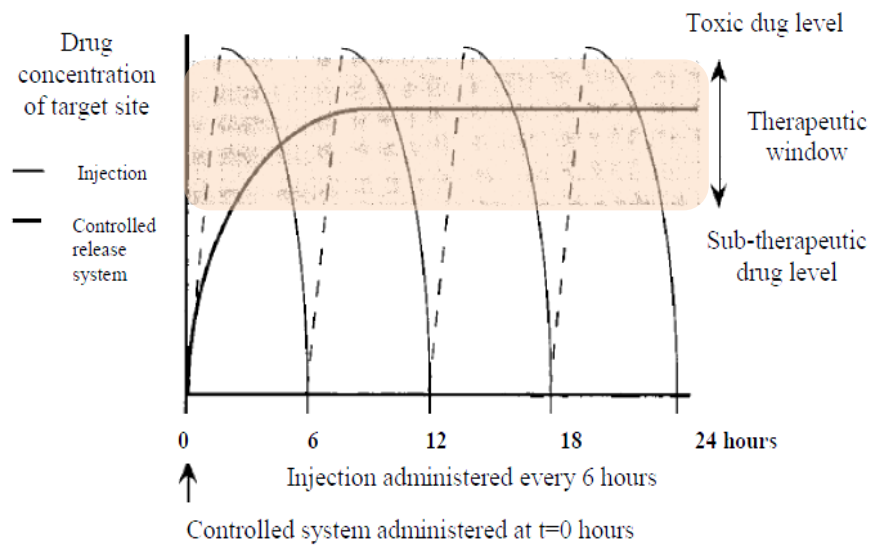
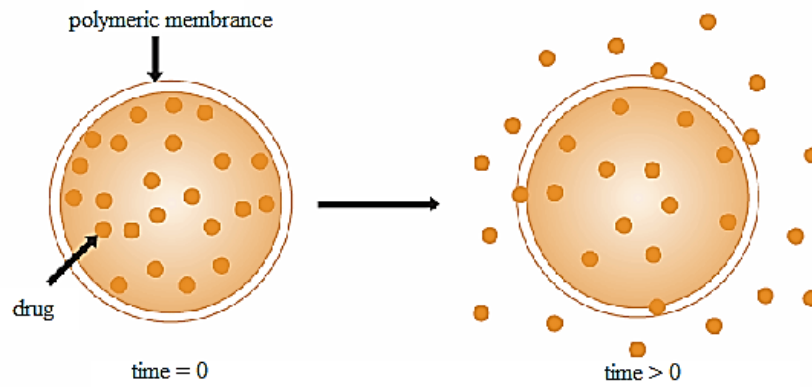


Figure 2.4 Drug concentrations at site of therapeutic action after delivery as a conventional injection (thin line) and as a temporal controlled release system

Controlled drug delivery occurs when a polymer is combined with the drug or other active agent in such a way that the active agent is released from the material in a predesigned manner [35].

a)



b)

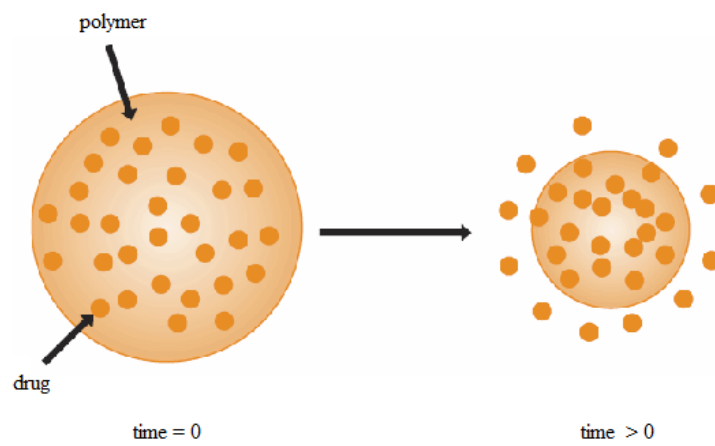


Figure 2.5 Representation of controlled release drug system [35]

a) reservoir diffusion b) biodegradable drug delivery device

2.3.1 Controlled release mechanisms

There are three mechanisms which active agents can be released from a delivery system [36].

1. Diffusion controlled delivery
2. Swelling controlled delivery
3. Degradation controlled delivery

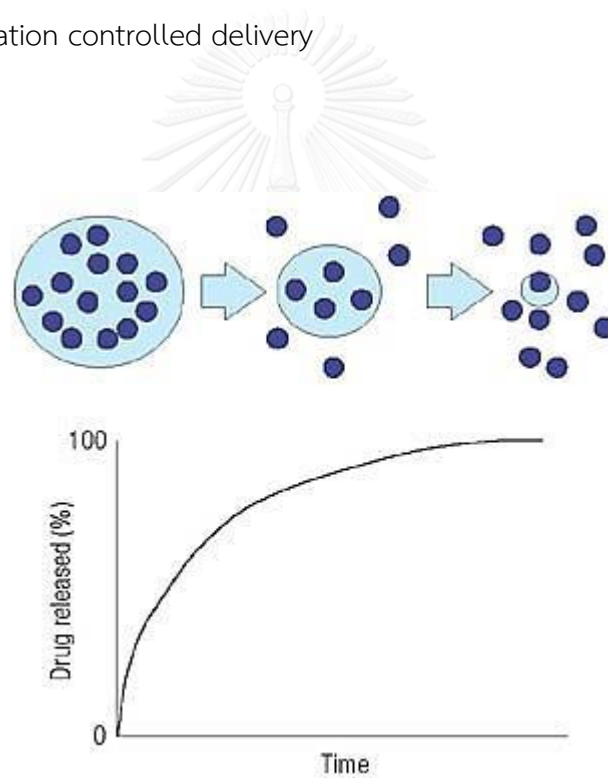


Figure 2.6 Drug delivery from carrier system [35]

In Figure 2.6, a polymer and active agent have been mixed to form a homogeneous system, also referred to as a matrix system. Diffusion occurs when the

drug passes from the polymer matrix into the external environment. As the release continues, its rate normally decreases with this type of system, since the active agent has a progressively longer distance to travel and therefore requires a longer diffusion time to release. For *the swelling* of the carrier increases the aqueous solvent content within the polymer matrix, enabling the drug to diffuse through the swollen network into the external environment. The swelling can be triggered by a change in the environment surrounding such as pH, temperature, ionic strength, etc.

2.4 Mucoadhesive system

In the 1980s, the mucoadhesive system was presented under the controlled drug delivery system. Mucoadhesives are synthesized to drug carrier for the residence time at the absorption site. This system is called mucoadhesive delivery system and the advantage of system has follow by

1. Increase in drug bioavailability due to first pass metabolism avoidance.
2. Improved patient compliance-ease of drug administration.
3. Prolongs the residence time of the dosage form at the site of absorption.
4. Due to an increased residence time it enhances absorption and hence the therapeutic efficacy of the drug.

2.4.1 Mechanisms of mucoadhesion

The mucoadhesive must contact the mucus membrane and increase surface contact and diffusible functional site within the mucus. Mucus is a complex viscous adherent secretion which is synthesized by specialized goblet cells. Mucus is composed of water and mucins, which are glycoproteins of high molecular weight. Moreover, pendant sialic acid on the glycoprotein molecules result in mucin behaving as an anionic polyelectrolyte at neutral pH [37]. Mucoadhesive delivery systems began to be various mechanism of mucoadhesion (Figure 2.7)

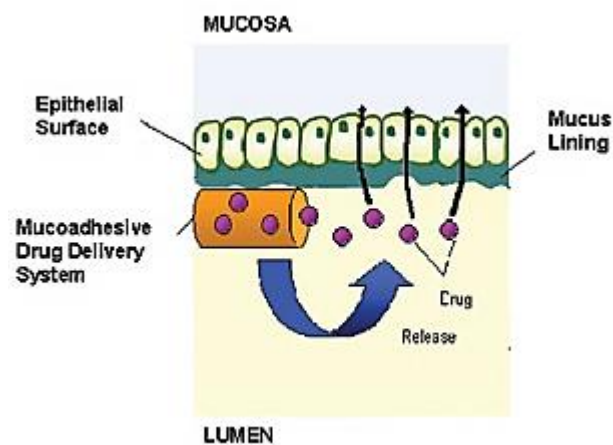


Figure 2.7 Mechanism of mucoadhesion [38]

The mechanism of mucoadhesion is generally divided into two steps are shown in Figure 2.8 [38].

The first stage (also known as contact stage), the contact between the mucoadhesive polymer and mucous membrane, with spreading and swelling of the formulation, initiating its deep contact with the mucus layer.

The second stage (the consolidation stage), the mucoadhesive materials are activated by the presence of moisture. Moisture plasticizes the system, allowing the mucoadhesive molecules to break free and to link up by weak vander waals and hydrogen bond.

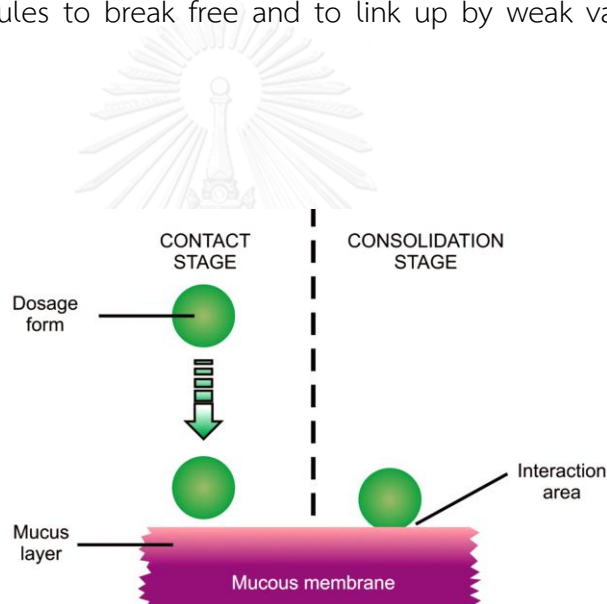


Figure 2.8 The two stages of the mucoadhesion process [39]

2.4.2 Mucoadhesion theories

There are six general theories have been proposed which can improve understanding for the phenomena of adhesion and can also be extended to explain the mechanism of bioadhesion. The theories include [38, 39]:

2.4.2.1 Electronic Theory

Electronic theory is based on the premise that both mucoadhesive and biological materials possess opposing electrical charges. Thus, when both materials come into contact, they transfer electrons leading to the building of a double electronic layer at the interface, where the attractive forces within this electronic double layer determines the mucoadhesive strength.

2.4.2.2 Wetting Theory

The wetting theory applies to liquid systems which present affinity to the surface in order to spread over it. This affinity can be found by using measuring techniques such as the contact angle. The general rule states that the lower the contact angle then the greater the affinity (Figure 2.9).

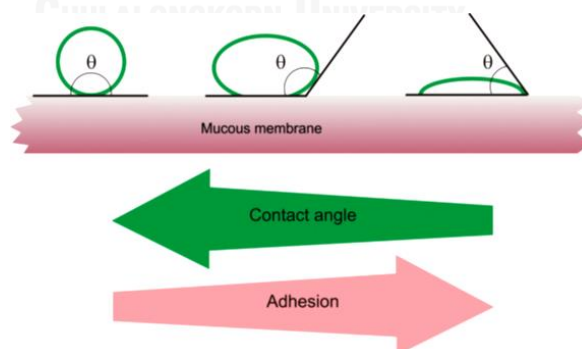


Figure 2.9 Schematic diagram showing influence of contact angle between device and mucous membrane on bioadhesion [39].

2.4.2.3. Adsorption Theory

According to the adsorption theory, the mucoadhesive device adheres to the mucus by secondary chemical interactions, such as in vander waals and hydrogen bonds, electrostatic attraction or hydrophobic interactions. For example, hydrogen bonds are the prevalent interfacial forces in polymers containing carboxyl groups. Such forces have been considered the most important in the adhesive interaction phenomenon because, although they are individually weak, a great number of interactions can result in an intense global adhesion.

2.4.2.4. Diffusion Theory

This theory assumes the diffusion of the polymer chains, present on the substrate surfaces shown in Figure 2.10, across the adhesive interface thereby forming a networked structure.

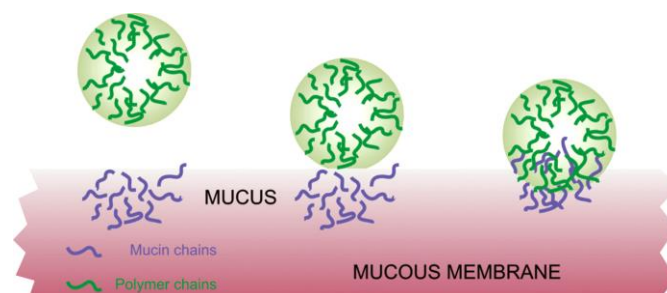


Figure 2.10 Secondary interactions resulting from interdiffusion of polymer chains of bioadhesive device and of mucus [39].

2.4.2.5. Mechanical Theory

Mechanical Theory explains the diffusion of the liquid adhesives into the micro-cracks and irregularities present on the substrate surface thereby forming an interlocked structure which gives rise to adhesion.

2.4.2.6. Cohesive Theory

This theory proposes that the phenomena of bioadhesion are mainly due to the intermolecular interactions amongst like-molecules. However, none of these mechanisms or theories alone can explain the mucoadhesion which occurs in an array of different situations.

2.4.3 The mucoadhesive/mucosa interaction

As mentioned above, bioadhesion may take place either by physical or by chemical interactions. For adhesion to occur, molecules must bond across the interface. These bonds can arise in the following way [39].

2.4.3.1. Physical interactions

- Hydrogen bonds

A hydrogen atom, when covalently bonded to electronegative atoms such as oxygen, fluorine or nitrogen, carries a slight positively charge and is therefore is

attracted to other electronegative atoms. The hydrogen can therefore be thought of as being shared, and the bond formed is generally weaker than ionic or covalent bonds.

- Vander waals bonds

The Vander waals bonds are some of the weakest forms of interaction that arise from dipole–dipole and dipole-induced dipole attractions in polar molecules, and dispersion forces with non-polar substances.

- Hydrophobic bonds

Hydrophobic bond that occur when non-polar groups are present in an aqueous solution. Water molecules adjacent to non-polar groups form hydrogen bonded structures, which lowers the system entropy. There is therefore an increase in the tendency of non-polar groups to associate with each other to minimise this effect.

2.4.3.2. chemical interactions

- Ionic bonds

The interaction between two oppositely charged ions via electrostatic interactions (e.g. in a salt crystal).

- Covalent bonds

Electrons are shared, in pairs, between the bonded atoms in order to “fill” the orbitals in both. These are also strong bonds (*e.g.* thiomer).

2.4.4 Mucoadhesive polymers

Mucoadhesive polymers may provide an important tool to improve the bioavailability of the active agent by improving the residence time at the delivery site. Mucoadhesive polymer have been also used for coating medical devices. As an example a new generation of intestine inspection device has been recently developed in which mucoadhesive polymer coating make intestinal locomotion possible.

These polymers can be subdivided into three classes: cationic, anionic and nonionic.

-Cationic polymers such as chitosan can electrostatic interact with the negatively charged mucus surface at physiological pH.

-Anionic polymers, including carboxymethylcellulose and alginates. The alginates, negatively charged polysaccharides, are widely used in the production of microparticles and are frequently reported as polyanionic mucoadhesive polymers. Synthetic polymers derived from poly(acrylic acid)(carbomers) has been considered

as a good mucoadhesive material with negatively charged and not water soluble but form viscous gels when hydrated such as polycarbophil.

-**Nonionic polymers**, including hydroxypropylmethylcellulose, hydroxyl ethylcellulose and methylcellulose, present weaker mucoadhesion force compared to anionic polymers

2.5 Technique to prepare micelles

The properties of PNPs have to be optimized depending on the particular application. In order to achieve the properties of interest, the mode of preparation plays a vital role. Thus, it is highly advantageous to have preparation techniques at hand to obtain PNPs with the desired properties for a particular application.

2.5.1 Methods for preparation of nanoparticles from dispersion of preformed polymer

Dispersion of drug in preformed polymers is a common technique used to prepare biodegradable nanoparticles from polymer. These can be accomplished by described Dialysis method.

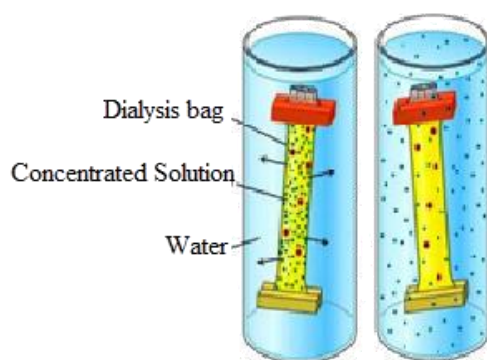


Figure 2.11 Schematic representation of dialysis method for preparation of polymeric micelles [40].

Dialysis offers a simple and effective method for the preparation of small, narrow-distributed polymeric micelles [40-44]. Polymer is dissolved in an organic solvent and placed inside a dialysis tube with proper molecular weight cut off. Dialysis is performed against a non-solvent miscible with the former miscible. The displacement of the solvent inside the membrane is followed by the progressive aggregation of polymer due to a loss of solubility and the formation of homogeneous suspensions of nanoparticles. This advantage of dialysis method is:

1. Dialysis technique requires no complicated or expensive equipment.
2. Dialysis is effective in removing nearly all of the free drug with a sufficient number of changes of the dialyzing medium.

CHAPTER III

EXPERIMENTAL

3.1 Materials

3.1.1 Model drug

Simvastatin (SV) was obtained as a gift sample from. Silommedical Co., Ltd. (Thailand)

3.1.2 Polymer

Chitosan, food grade, Mw 500 kDa., Deacetylation 85 %, Lot No. 497613, (Seafresh, Thailand)

3.1.3 Chemicals

1. Methyl iodide: analytical grade; Sigma-Aldrich
2. *N*-methylpyrrolidone: analytical grade; Sigma-Aldrich
3. Gallic acid: analytical grade; Sigma-Aldrich
4. Stearic acid: analytical grade; Sigma-Aldrich
5. 1-Ethyl-3-(3-dimethylaminopropyl)carbodiimide: analytical grade; Sigma-Aldrich
6. Mucin from porcine stomach (type 2): analytical grade; Sigma Aldrich
7. Potassium dihydrogen phosphate: analytical grade; Merck
8. Potassium bromide: analytical grade; Merck
9. Potassium iodide: analytical grade; Merck
10. Sodium chloride: analytical grade; Merck
11. Sodium hydrogen phosphate: analytical grade; Merck
12. Sodium hydroxide: analytical grade; Merck
13. Sodium tripolyphosphate: analytical grade; Sigma-Aldrich

14. Potassium hydroxide: analytical grade; Lab-Scan
15. Acetone, commercial grade; Merck
16. Acetic acid: AR grade; Union chemical
17. Hydrochloric acid fuming 37%: analytical grade; Merck
18. Ethanol 95 %: commercial grade; Merck
19. Dialysis membrane with *M_w* cut off at 12,000 – 14,000 Da; Sigma-Aldrich

3.2 Instruments

Table 3.1 The Instruments used in this study

Instrument	Manufacture	Model
FTIR spectrometer	Nicolet	6700
NMR spectrometer	Varian	400MHz
Freeze dryer	Labconco	Freeze 6
UV-VIS spectrometer	Perkin Elmer	Lambda 80
Scanning Electron Microscope	Philips	XL30CP
Small bench centrifuge	Hettich	EBA20
Particle sizer	Malvern Instruments	S4700
Vortex	Vortex-genie	V2
Micropipette	Mettler Toledo	Volumate
Horizotal shaking water-bath	Lab-line instrument	3575-1

3.3 Methods

3.3.1 Synthesis of Stearate-gallate-*N*-trimethylchitosan

3.3.1.1 Synthesis of *N*-trimethylchitosan (TMC)

The synthesis of TMC in detail was reported previously [45]. A mixture of 100 mL of a 1% w/v chitosan, 60 mL of a 1:1 v/v methyl iodide/ *N*-methylpyrrolidone (NMP) and 5 mL of a 15% w/v aqueous sodium hydroxide solution was stirred on a water bath at a temperature of 60°C for 45 min. The methyl iodide was kept in the reaction. The product was precipitated with ethanol and isolates by centrifugation. After washing with ethanol, the product was dissolved in 40 mL of a 5% w/v aqueous sodium chloride solution to exchange the iodide ion with a chloride ion. The polymer was precipitated with ethanol. This product was dissolved in acetone to remove the remaining sodium chloride from the material.

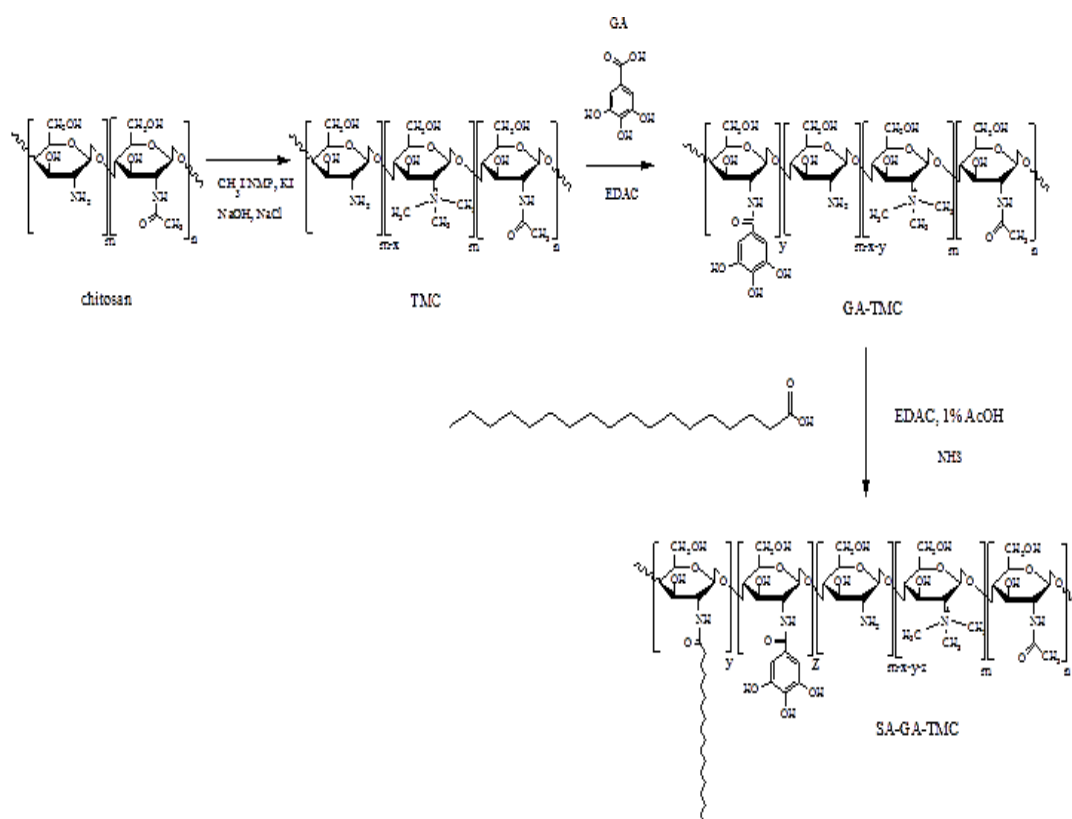
3.3.1.2 Synthesis of GA-TMC conjugate

TMC was synthesized from chitosan as per a procedure described in the literature with some modifications [46]. To a solution of gallic acid (0.38 g.) in water/ethanol (1:1, 20 mL), EDAC (0.43 g.) in 20 mL water was added with constant stirring. TMC (1.0 g.) was dissolved in 20 mL distilled water and added slowly to the

reaction mixture with constant stirring in an ice bath for 30 min., stirring was continued for another 24 h at room temperature. After completion of the reaction, reaction mixture was precipitated with acetone and dialyzed against distilled water to remove the byproducts and unreacted gallic acid. The resultant GA-TMC was dried by freeze dry.

3.3.1.3 Synthesis of SA-GA-TMC conjugate

The SA-GA-TMC conjugate was synthesized via the reaction of carboxy groups of stearic acid (SA) with amine groups of CS in the presence of EDC. GA-TMC was fully dissolved (0.01 g/mL) in 1% (v/v) acetic acid at room temperature overnight to perform 20 mL GA-TMC solution. SA (0.1 g, 0.35 mmol), EDAC (0.34g, 1.76 mmol), and NHS (0.20 g, 1.76 mmol) were dissolved in 7 mL of an ethanol/acetone mixture (ethanol/acetone = 2/5 (v/v)) and then heated at 60 °C for 1 h. The solution was added into the GA-TMC solution, followed by stirred and refluxed for another 24 h. Finally, the reaction solution was dialyzed against distilled water for 1 day using a dialysis membrane to remove excess EDC and NHS and lyophilized at -44 °C and 0.01 mbar. Then the lyophilized product was further purified with ethanol to remove byproduct.



Scheme 3.1 Synthesis flowchart of Stearate-gallate-*N*-trimethylchitosan (SA-GA-TMC)

จุฬาลงกรณ์มหาวิทยาลัย
CHULALONGKORN UNIVERSITY

3.3.2 Chemical characterization

3.3.2.1 Fourier transformed infrared spectroscopy (FT-IR)

The CS, TMC, GA-TMC and SA-GA-TMC were prepared as potassium bromide pellets. FTIR spectra were performed by a Nicolet 6700 Fourier transform infrared (FTIR) spectrometer in the region from 4000 to 400 cm⁻¹.

3.3.2.2 ^1H Nuclear Magnetic Resonance spectroscopy (^1H NMR)

^1H NMR spectra were recorded on Bruker NMR spectrometer operated at 400 MHz. $\text{D}_2\text{O}/\text{CF}_3\text{CO}_2\text{H}$ (1%, v/v) was used to dissolve 5 mg of chitosan and modified chitosan (TMC, GA-TMC and SA-GA-TMC). The degree of quaternization of chitosan was determined by ^1H NMR spectroscopy according to Eq. (1). In order to the substitution of GA and SA were determined by ^1H NMR spectroscopy according to Eq. (2, 3) respectively.

$$\% DQ = \left[\frac{I_{(\text{CH}_3)_3}}{I_{(\text{H}_3-\text{H}_6)}} \times \frac{5}{9} \right] \times 100 \quad \text{..... (1)}$$

where $I_{(\text{CH}_3)_3}$ is the integral of the trimethyl protons of the trimethyl chitosan and $I_{(\text{H}_3-\text{H}_6)}$ is the integral of the methyl protons (H3, H4, H5 and H6) of chitosan.

$$\% DS_{GA} = \left[\frac{I_{(\text{Ha})}}{I_{(\text{H}_3-\text{H}_6)}} \times \frac{5}{2} \right] \times 100 \quad \text{..... (2)}$$

$$\% DS_{SA} = \left[\frac{I_{(\text{CH}_2)_{16}\text{CH}_3}}{I_{(\text{H}_3-\text{H}_6)}} \times \frac{5}{35} \right] \times 100 \quad \text{..... (3)}$$

where $I_{(\text{Ha})}$ is the integral of protons of the gallic acid and $I_{(\text{CH}_2)_{16}\text{CH}_3}$ is the integral of methyl protons of the stearic acid.

3.3.2.3 Critical Micelle Concentration (CMC) determination

The critical micelle concentration (CMC) of the synthesized CS-SA was estimated by fluorescence spectroscopy using pyrene. Then, 0.25 g of SA-GA-TMC was prepared in 25 mL water and diluted to different concentrations from 5.0×10^{-7} to 1.0 mg/mL. 20 μL of pyrene solution was added in 2.0 mL of each polymer concentrations and vortexed for 5 min. Then the ratio of the intensities (I_1/I_3) of the first peak (I_1 , 374 nm) to the third peak (I_3 , 384 nm) was determined.

3.3.3 In vitro bioadhesion of mucin to chitosan and modified chitosan

(a) Mucus glycoprotein assay

The Periodic Acid Schiff (PAS) colorimetric method is widely used for analysis of mucins, glycoproteins and other polysaccharides in tissues and cells [47]. The PAS colorimetric assay used for the detection of the free mucin concentration for the studies on the adsorption of mucin on CS, TMC, GA-TMC and SA-GA-TMC. Two reagent were prepared. Schiff reagent contained 1% (w/v) basic fuchsin (pararosaniline) dissolved in DI water. 20 mL of 1 M HCl and 0.1 g of Sodium metabisulphite was added to every 6 ml of fuchsin solution. The resulting solution was incubated at 37°C until it became pale yellow. The solution was filtered before use. Periodic acid reagent was freshly prepared by adding 10 μL of 50% (v/v) periodic acid solution to 7 mL of 7% (v/v) acetic acid solution.

Standard calibration curves were prepared from 2 ml of mucin standard solutions (0.025-0.5 mg/mL). After adding 100 μ L of periodic acid reagent, the solutions were incubated at 37 °C for 2 h. Then, 100 μ L of Schiff reagent was added at room temperature for 30 min. 100 μ L aliquots of the solution were transferred in triplicate into a 96-well microtiter plate and the absorbance at 555 nm was recorded.

(b) Adsorption of mucin on chitosan and modified chitosan (TMC, GA-TMC and SA-GA-TMC)

A 0.5% (w/v) mucin solution in each of three broadly isoosmotic solutions that differ in pH, namely SGF (pH 1.2), 0.1 M sodium acetate buffer (pH 4.0), 0.1 N phosphate buffer (pH 5.5) and SIF (pH 6.4) media, were prepared. CS and its three conjugates were dispersed (at 20 mg/1.5 mL final) in the above mucin solutions, vortexed, and shaken at 37°C for 2 h. Then the dispersions were centrifuged at 12000 rpm for 2 min to the CS-mucin, TMC-mucin, GA-TMC-mucin and SA-GA-TMC-mucin complex and the supernatant was harvested and used for the measurement of the free mucin content. The mucin concentration was calculated by reference to the calibration curve, and the amount of mucin absorbed to the microspheres was calculated as the difference between the total amount of mucin added and the free mucin content in the supernatant.

3.4 Pharmaceutical applications

In order to study a pharmaceutical application potential of SA-GA-TMC micelles as a drug delivery system. The SA-GA-TMC micelles were prepared in aqueous solution using simvastatin (SV) as a coronary heart drug is the representation model drug for studying the drug delivery system. The properties of drug loaded micelles, e.g. morphology, particle size, zeta potential, encapsulation efficiency, drug loading and drug release profiles were investigated.

3.4.1 Preparation of drugs-loaded SA-GA-TMC micelles

SV loaded SA-GA-TMC (SA-GA-TMC/SV) micelles were prepared by a membrane dialysis method. First, 50 mg of SA-GA-TMC was dissolved in 50 mL of DI water, followed by addition of 5mL of SV solution (1 mg/mL). The mixture was vortexed and then dialysis against deionized water at room temperature for 24 h using a dialysis membrane (molecular weight cut-off of 3500 g mol⁻¹). The product was centrifuged at 3000 rpm for 8 min to remove precipitated drug and the final product was obtained. As a control, SA-GA-TMC micelles without SV were also prepared.

3.4.2 Characterization of the SA-GA-TMC micelles

3.4.2.1 Scanning Electron Microscope (SEM)

The SA-GA-TMC (0.2, 0.4, 0.6, 0.8, 1.0 and 1.4 mg) was dispersed completely in 1 mL DI at room temperature and the solutions were shaken by high vortex for 2 h. The solutions were the dropped onto the clean surface of a glass slide for self-assembly for 2 d. The samples were mounted onto an aluminum stub using double-sided carbon adhesive tape and coated with gold-palladium. The morphologies were observed via scanning electron microscope under high vacuum at an ambient temperature with a beam voltage of 10-20 kV.

3.4.2.2 Particle size measurement

The particle size and size distribution of microspheres were evaluated with a particle size analyzer (Zetasizer nano series, Malvern instruments). The CS, TMC, GA-TMC, SA-GA-TMC micelles and SA-GA-TMC/SV micelles with the concentration of 1 mg/mL CS-SA were performed using a Zetasizer analyzer. Size calculation was based on dynamic light scattering (DLS) method as a software protocol. The scattered light was collected at an angle of 90° through fiber optics and converted to an electrical signal by an avalanche photodiode (APDS). All sample were sonicated and run in triplicate with the number of runs set to 5 and run duration set to 10 seconds. All measurements were performed in triplicate.

3.4.2.3 Zeta potential

Zeta potential of the microspheres was determined using particle sizer. The analysis was performed at a scattering angle of 90°. All samples were sonicated and run in triplicate with the number of runs set to 5 and run duration set to 10 seconds. All measurements were performed in triplicate.

3.4.2.4 Fourier Transform Infrared (FTIR) Spectroscopy

The FTIR spectra of the pure drug and drug loaded microspheres were examined by using the potassium bromide disk (KBr) method with a Fourier transform infrared (FTIR) spectrometry in the range of 4000-400 cm^{-1} .

3.4.3 Study of the drug behavior of the micelles

3.4.3.1 Calibration curve of SV

The standard stock SV solution was prepared in 1% (v/v) EtOH. SV 5 mg was accurately weighted and dissolved with 1% (v/v) EtOH into 50 mL volumetric flask and adjusted to volume (100 ppm).

The stock SV solution was diluted to 3, 6, 9, 12, 15 and 18 ppm with 1% (v/v) EtOH in volumetric flask.

The absorbance of standard solution was determined by UV-Vis spectrophotometer at 238 nm. The 1% (v/v) EtOH was used as a reference solution.

The absorbance and calibration curve of SV in 1% (v/v) EtOH was shown in Appendix A.

3.4.3.2 Calibration curve of SV in pH 1.2, 4.0 and 6.4

The standard stock SV solution was prepared in 1% (v/v) EtOH in pH 1.2, 4.0 and 6.4. SV 5 mg was accurately weighted and dissolved with 1% (v/v) EtOH into 50 mL volumetric flask and adjusted by various buffers to volume (100ppm).

The stock SV solution was diluted to 3, 6, 9, 12, 15 and 18 ppm with three different buffers in volumetric flask.

The absorbance of standard solution was determined by UV-Vis Spectrophotometer at 238 nm. The 1% (v/v) EtOH was used as a reference solution. The absorbance and calibration curve of SV in 1% (v/v) EtOH was shown in Appendix B.

3.4.3.3 Determination of encapsulation and drug loading efficiency (%EE)

To determine the SV encapsulation and drug-loading efficiency, 1 mg of SV-loaded micelles was dissolved in 1 mL of water. This solution was then analyzed by an ultraviolet (UV) spectrophotometer at 238 nm with SA-GA-TMC solution as the control. The drug concentration in the solution was calculated based on the standard curve. The drug encapsulation efficiency (EE) and drug-loading ratio (DL)

were obtained in accordance with the following equation. All measurements were performed in triplicate.

$$EE \% = \left(\frac{\text{amount of drug loaded in the micelles}}{\text{amount of drug added during fabrication}} \right) \times 100\%$$

$$DL \% = \left(\frac{\text{amount of drug loaded in the micelles}}{\text{the total amount of drug in the micelles and SA-GA-TMC used in the process}} \right) \times 100\%$$

3.4.3.4 In vitro drug release

In vitro release studies of SV from SA-GA-TMC micelles were performed using buffers pH 1.2, 4.0 and 6.4 (SGF, vaginal fluids and SIF, respectively) at $37 \pm 1^\circ \text{C}$ by dialyzing 2 mL of an aqueous solution of SV-loaded SA-GA-TMC micelles (1 mg/mL) against 50 mL of the appropriate buffer in a flask. The flask was placed in a shaken water bath at speed of 100 rounds per minutes and incubated $37 \pm 1^\circ \text{C}$.

The 3 mL samples were withdrawn at specified time intervals (at 0, 5, 10, 15, 30, 45 minute 1, 2, 3, 4, 5, 6, 7, 8 and 24 hours, respectively). An equal volume of fresh dissolution medium was placed to maintain the volume constant. The released SV were analyzed by UV-Vis spectrophotometer at 238 nm.

The amount of SV released was calculated by interpolation from a calibration curves containing increasing concentrations of SV. The percentages of cumulative SV release were calculated from this equation.

$$\% \text{ Cumulative release} = \left(\frac{\text{Amount of SV from release}}{\text{A mount of SV before release}} \right) \times 100$$

3.4.4 Statistical analysis

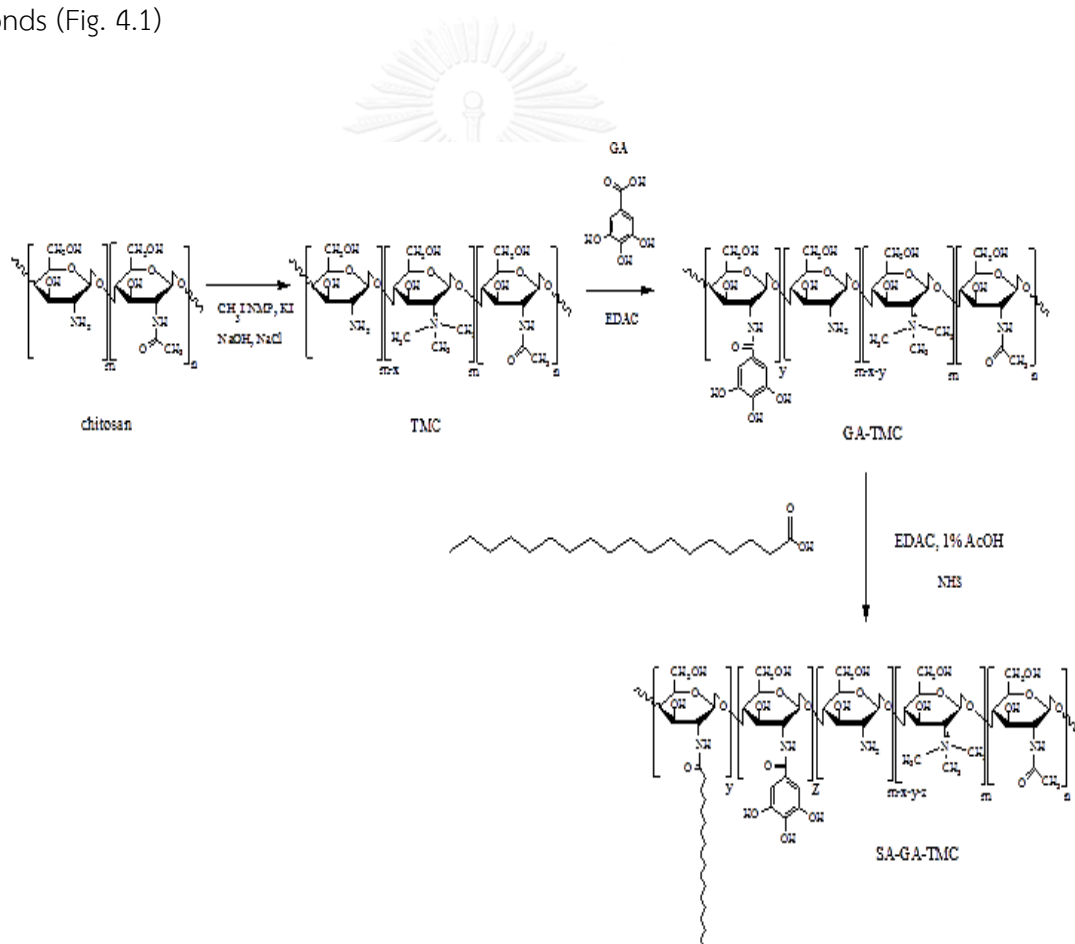
All measurements were performed in experiment. Results are presented as mean \pm SD. Statistical analysis was performed by one-way ANOVA using Microsoft Excel (Microsoft Corporation) with P<0.05 considered to indicate statical significance.

CHAPTER IV

RESULTS AND DISCUSSION

4.1 Synthesis of TMC, GA-TMC AND SA-GA-TMC

The first step, the reaction of CS to form *N*-trimethylchitosan by methyl iodide was attacked with the amino groups of CS [45]. The second step, the GA and SA were covalently reacted at the amino groups of CS via the formation of amide bonds (Fig. 4.1)



Scheme 4.1 Synthesis flowchart of stearate-gallate-*N*-trimethyl chitosan (SA-GA-TMC).

4.2 Characterization and physical properties of chitosan, N-trimethylchitosan, gallate-N-trimethylchitosan and stearate-gallate-N-trimethyl chitosan

4.2.1 Fourier transformed infrared spectroscopy (FT-IR)

The FTIR spectra of CS, TMC, GA-TMC and SA-GA-TMC are shown in Figure 4.2. The FTIR spectra of CS and TMC are consistent with those of previously reported [48]. After conjugated GA onto the C2-amine groups of chitosan, the characteristic showed dramatically increasing a broad absorption at 3200-3590 cm^{-1} (Figure 4.2c). It was assigned to the stretching vibration of the O-H of GA, and a new peak occurred at 1560 cm^{-1} (amide II band), suggesting that the conjugation of GA on TMC (via the formation of amide linkage). The peak at 1639 cm^{-1} assigned to C=O of secondary amide slightly overlapped to the C=C aromatic ring of GA at 1639 cm^{-1} (Figure 4.2c). In addition, the spectrum of conjugated SA onto the CS backbone (Figure 1d) showed absorption peak at 1639 and 1560 cm^{-1} were attributed to the amide C=O stretching and secondary amine of SA-GA-TMC, respectively. The absorption band at 1470 cm^{-1} attributed to CH_2 and CH_3 deformation of SA. An increase of the intensity band at 2851-2929 cm^{-1} range assigned to axial deformation of C-H bonds, due to present of long chain hydrocarbons. In order to it can observed peak at 1705 cm^{-1} assigned to C=O of carboxyl group, indicated that the successful preparation of SA-GA-TMC conjugation.

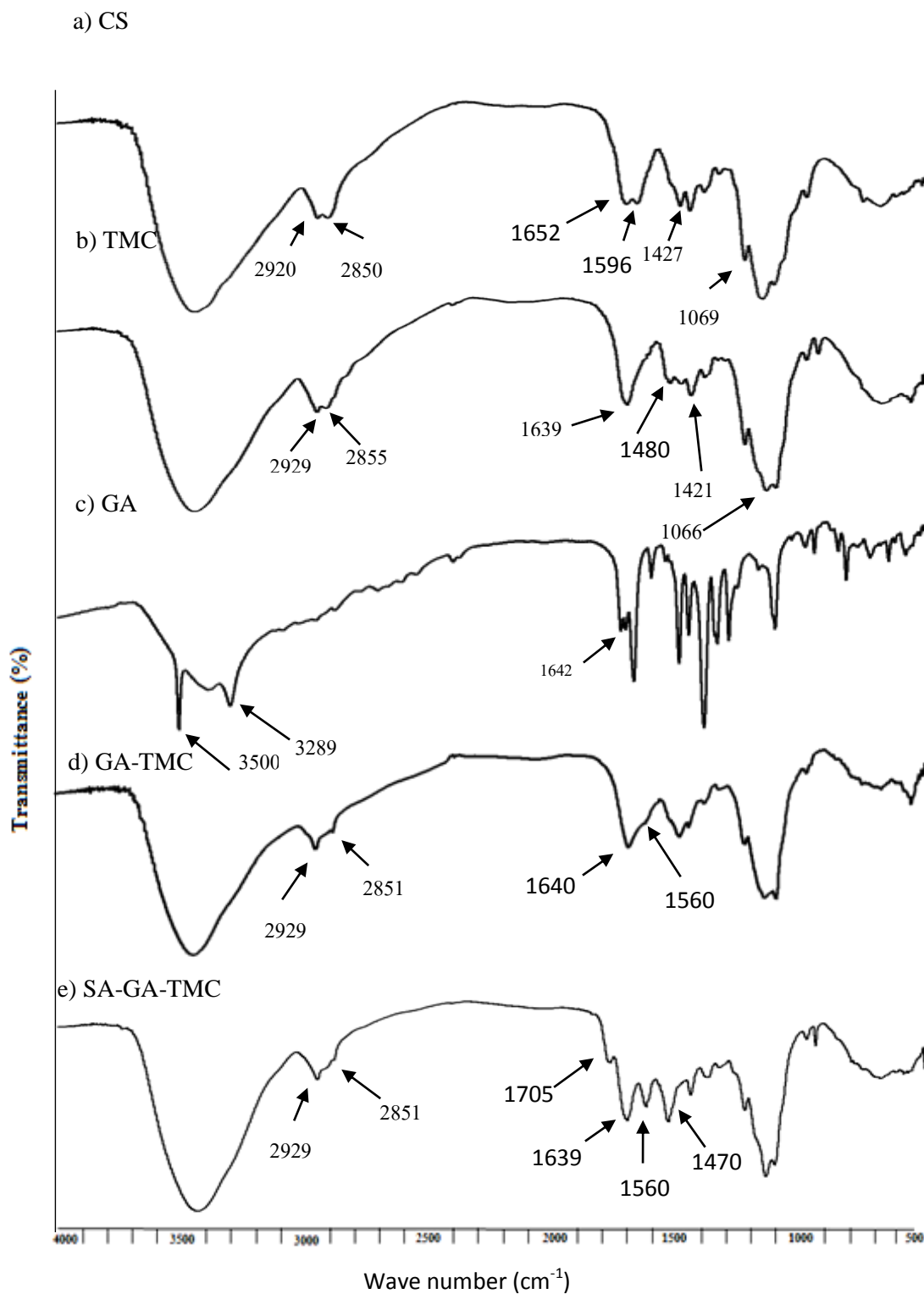
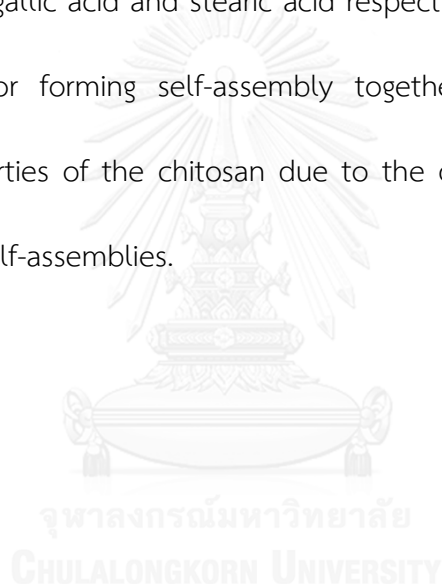


Figure .4.2 FTIR spectra of CS (a), TMC (b), GA (c), GA-TMC (d) and SA-GA-TMC (e).

4.2.2 ^1H Nuclear Magnetic Resonance spectroscopy (^1H NMR)

The chemical structures of chitosan and modified chitosan (TMC, GA-TMC and SA-GA-TMC) were characterized by ^1H NMR as shown in Figure 4.3. The peak at chemical shifts of 4.42, 3.40-3.98, 3.03 and 1.92 ppm were ascribed to the H1, H3-H6, H2 and acetyl protons in the chitosan skeleton (Figure 4.3a), respectively. The appearances of new proton positions from dimethyl amino group and trimethyl amino group were observed at 2.69 and 2.88 ppm, respectively. As evident from the enlargement of the peaks assigned to the quaternary amino groups (Figure 2b), as well as at 3.14 ppm for O-methylated group. Furthermore, the peaks at 3.03 ppm attributed to the H at carbon 2 and 1.98 ppm (s, 3H) for the acetyl protons of GluNAc units. The ^1H NMR spectra of GA, a proton singlet at 7.12 ppm relates to the protons on aromatic ring. After conjugate the results of the spectra of the GA-TMC conjugate showed the proton of aromatic ring at chemical shift 8.00 ppm (Figure 2c) that was shifted from 7.12 ppm. It was assigned to the Ha (Aromatic proton) of the GA. In order to the spectra of SA-GA-TMC showed the appearances of new proton position of the long chain hydrocarbon showed at 2.38 ppm for H of $-\text{CH}_2\text{CO}-$, at 2.30 ppm for H of $\text{CH}_2\text{CH}-$ and peak at 0.88 ppm for H of $-\text{CH}_3$ (Figure 2d). The result support that the SA-GA-TMC were successfully synthesized.

The degree of quaternization (%DQ) of chitosan and the degree of substitution (%DS) of gallic acid and stearic acid are consistent with those of previously reported [49, 50] by ^1H NMR spectroscopy. The degree of quaternization of chitosan were determined by ^1H NMR spectroscopy according to Eq.1. In order to the substitution of GA and SA were determined by ^1H NMR spectroscopy according to Eq. (2, 3) respectively, it was found to be 24.33 ± 0.18 (%DQ) and 5.00 ± 0.02 (%DS) and 21.77 ± 0.07 (%DS) of gallic acid and stearic acid respectively, which may influence to develop structure for forming self-assembly together along with enhance the mucoadhesive properties of the chitosan due to the chemical structure influences the morphology of self-assemblies.



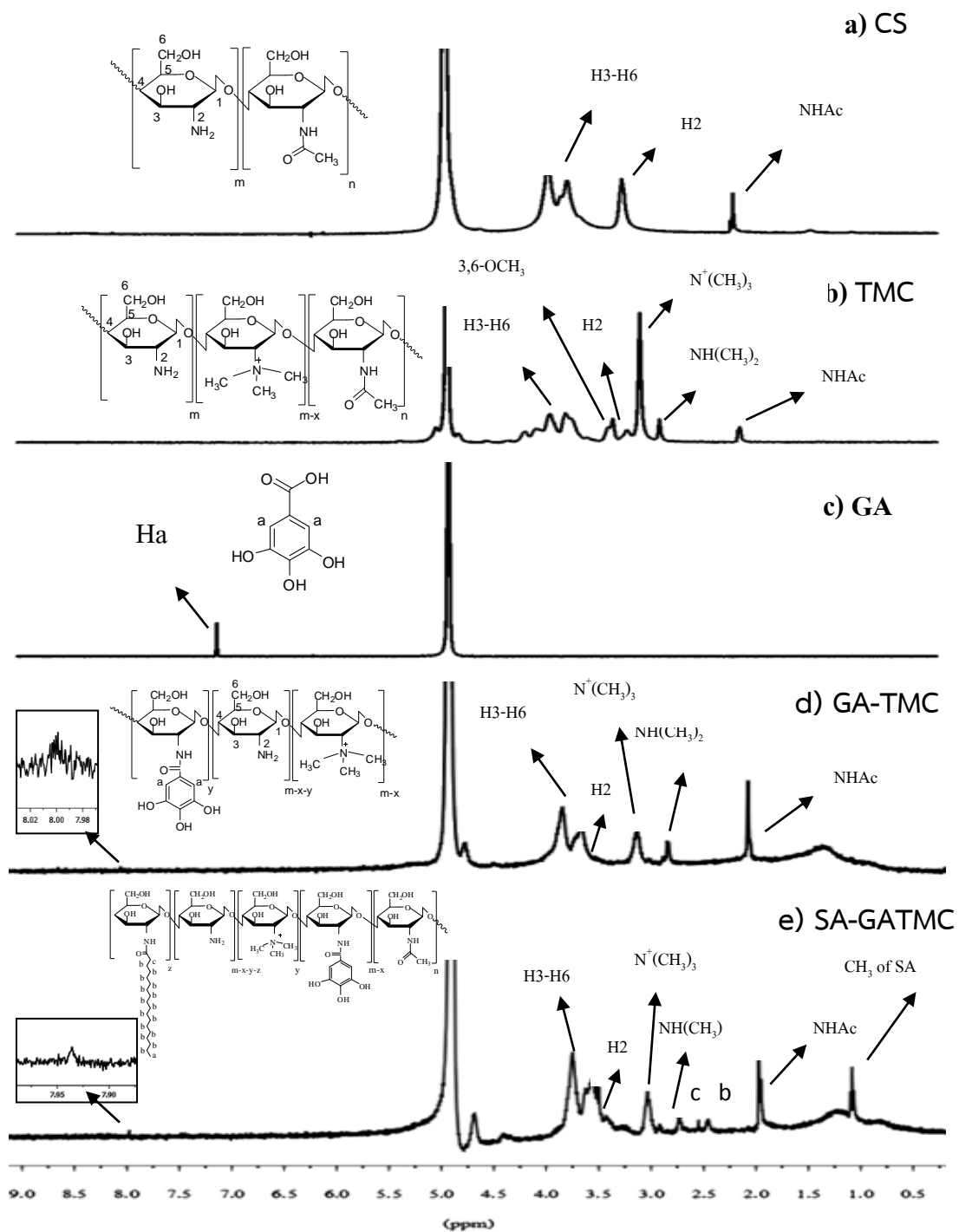


Figure.4.3 Representative ^1H NMR spectra of (a) CS, (b) TMC, (c) GA, (d) GA-TMC and (e) SA-GA-TMC.

4.3 Self-Assembly Morphologies

There are a large number of factors, including chemical structure, self-assembly time and solvent, which may influence the morphology of self-assemblies [51]. In this work, the effects of speed, time and concentration on self-assemblies.

The SA-GA-TMC dispersed completely in 1 mL DI at room temperature and the solutions were shaken by high vortex for 2 h. The solutions were the dropped onto the clean surface of a glass slide for self-assembly for 2 d. The morphological appearance of SA-GA-TMC was self-assembly cubical shape (Figure 3.) by scanning electron microscope. This might be due to the SA-GA-TMC micelles were subdivided by high vortexing to form small spherical micelles. The solutions of small micelles were dropped onto a glass slide freeze dried in vacuum for 2 days.

4.3.1 Effects of speed and time on self-assembly

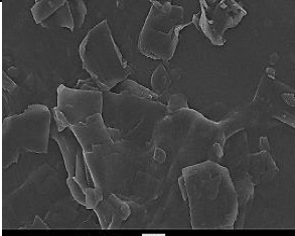
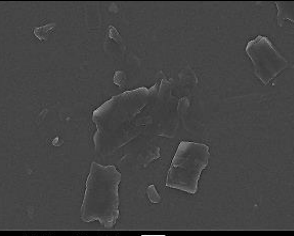
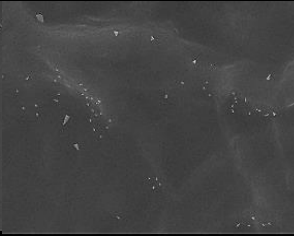
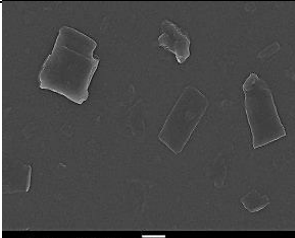
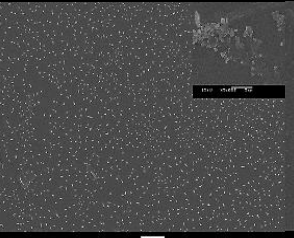
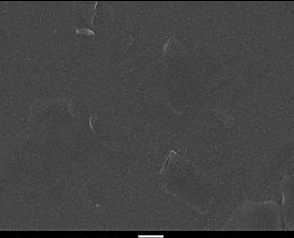
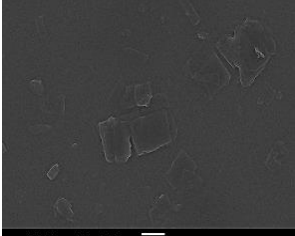
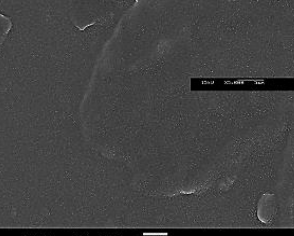

With the increase of speed and time in prepare self-assemblies were analyzed by scanning electron microscopy (SEM). The morphological appearance of SA-GA-TMC was self-assembly cubical shape.

As in Figure 3, it was found that the sizes of SA-GA-TMC micelles decreased with increasing the speed. Due to the increasing speed from 1700 to 3100 rpm, the SA-GA-TMC micelles were performed by external force until breaking in polymer

chains by increasing speed of vortexing. Then the polymer chains were also able to form particles. This is the evidence for the small particles sizes of SA-GA-TMC at 3100 rpm of speed (1 h). According to the results, we found that the sizes of SA-GA-TMC micelles decrease as the time on self-assembly increased for each speed of vortexing. Due to the increasing time on self-assembly from 1 to 3 h, the SA-GA-TMC micelles were increasingly subdivided for long time on self-assembly become to small particles sizes at 3 h. We hypothesized that the small micelles onto a glass slide need stability on the surface micelles aggregated to form self-assembly association in limited area by random walk theory [52, 53]. Then the micelles were rearranged to form nanocubic micelles via $\pi - \pi$ stacking of aromatic group of gallic acid.

However, the SA-GA-TMC micelles were prepared self-assemblies at 2 h and 2400 rpm suitable applications of SA-GA-TMC micelles for loading drug as a drug delivery system. Due to the shape with small particle sizes of about 0.4-0.7 μm .

Table 4.1 SEM images of prepared self-assemblies with various speed and time by vortexing of SA-GA-TMC concentration 1 mg/mL

Speed (rpm)	Time (h)		
	1	2	3
1700			
2400			
3100			

4.3.2 Effects of concentrations on self-assembly

We are presented study effects of concentrations by the SEM images of self-assemblies with various SA-GA-TMC concentrations (0.2, 0.4, 0.6, 0.8, 1.0 and 1.4 mg/mL) at 2 h and 2400 rpm for 2 days. Figure 4.4 presented the SEM images of self-assemblies with various SA-GA-TMC concentrations. With the increase of SA-GA-TMC

concentration for 2 days was analyzed by scanning electron microscopy (SEM). The morphological appearance of SA-GA-TMC was self-assembly cubical shape. The results of self-assemblies with various concentrations imply the capability of the self-assemblies. At low concentration (0.2 mg/mL), the particles size of SA-GA-TMC micelles have small particles size and spread around on the glass slide. Then the increasing concentration (0.4, 0.6, 0.8 and 1.0 mg/mL), it was found that the sizes of SA-GA-TMC micelles increased. Due to the increasing concentrations, the small particles on the surface aggregated to form cubical self-assemblies via $\pi - \pi$ stacking in limited area. In particular, with a high concentration of SA-GA-TMC (1.4 mg/mL) both disordered aggregated and particles are observed, probably due to the lack of space for self-assembly and aggregation of SA-GA-TMC micelles with excellent array sequence. Chemical analysis using energy-dispersive X-rays (EDX) showed major peaks for carbon and oxygen, suggested it is rich in both C and O with a weak peak due to silicon (Figure 4.5). No other elements were observed to be present. The silicon, sodium, magnesium, potassium and calcium peaks may come from the glass slide.

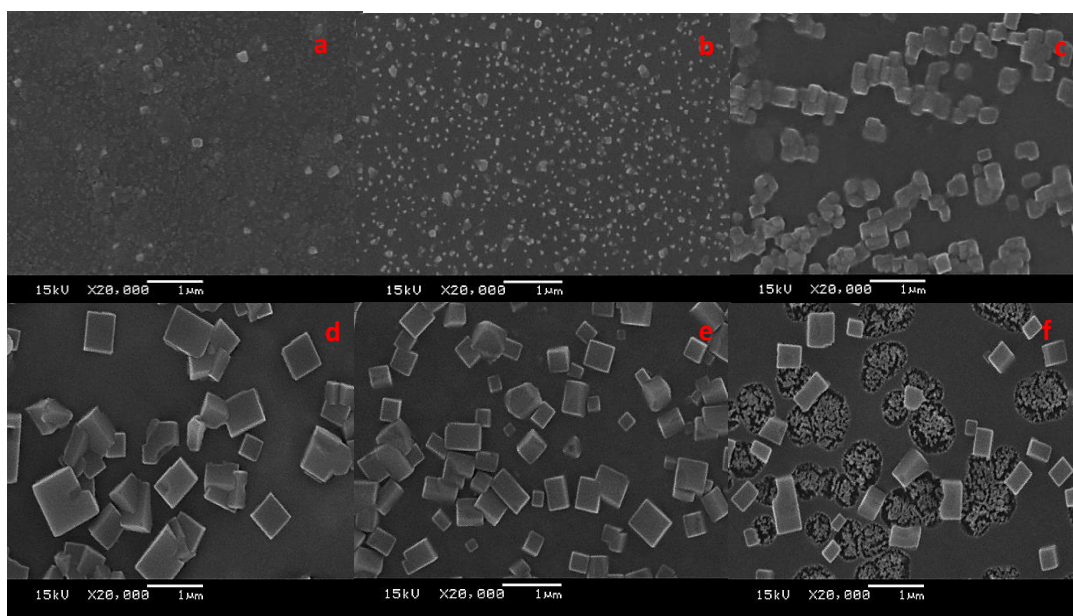


Figure 4.4. SEM images of self-assemblies with various SA-GA-TMC concentrations: a) 0.2, b) 0.4, c) 0.6, d) 0.8 e) 1.0 and f) 1.4 mg/mL at 2h and 2400 rpm for 2 d.

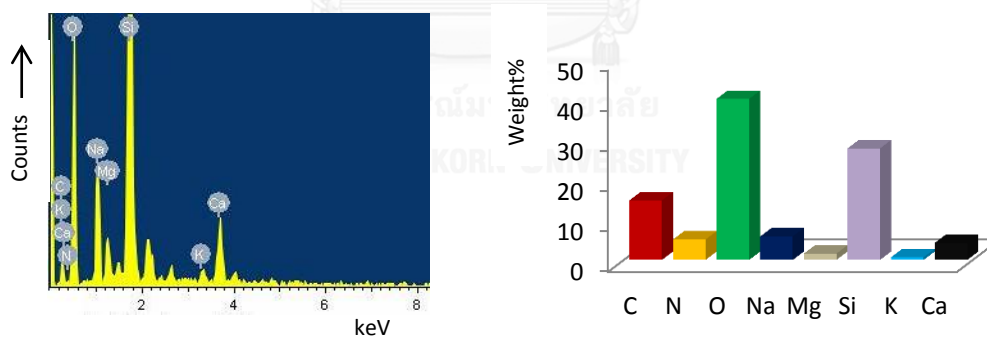


Figure 4.5. EDX spectrum of cubic self-assemblies of SA-GA-TMC (1mg/mL).

However, self-assembly cubic of SA-GA-TMC with a size between 0.4-0.7 μm was observed by self-assembling a SA-GA-TMC (1 mg)/ DI (1 mL) solution suitable applications of SA-GA-TMC micelles for loading drug as a drug delivery system. A

similar result has been observed and confirmed for the self-assembly of stearic acid- β -chitosan polymeric micelles [54].

4.3.3 Critical Micelle Concentration (CMC) determination

CMC was commonly used to describe the stability and physical property of micelles. Figure 4.6 presented the CMC of synthesized SA-GA-TMC was estimated by fluorescence spectroscopy using pyrene as a probe.

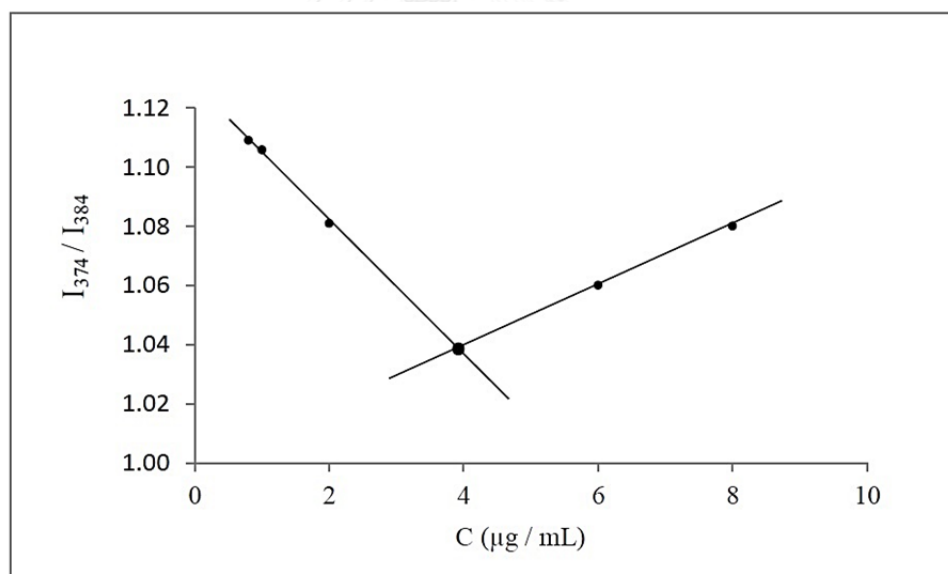


Figure 4.6 Plot of intensity ratio I_{374}/I_{384} as polymer concentrations.

The CMC value of SA-GA-TMC was found at 3.98 $\mu\text{g}/\text{mL}$. As a result, the SA-GA-TMC form through self-assembly at a low concentration. It is outstandingly for polymeric micelles due to the fact that polymeric micelles exhibit lower CMC, which offer greater resistance toward dissociation upon dilution in the GI tract.⁸

4.4 Mucoadhesive properties

4.4.1 Assessment of the mucoadhesive behavior of CS, TMC, GA-TMC and SA-GA-TMC by mucus glycoprotein assay

In this study, porcine mucin type II was selected which is typically used in mucoadhesion assays due to its lower batch-to-batch variability and higher between assay reproducibility [11]. As a strong interaction exists between mucin and CS or its derivatives, mucin should be spontaneously adsorbed onto the surface of the CS or its derivatives.

Periodic acid: Schiff (PAS) colorimetric method was used to qualify mucin conjugated polymer bioadhesed strength [55, 56] in the simulated gastrointestinal fluid in pH 1.2 (SGF), pH 4.0 and pH 6.4 (SIF) that a strong interaction exists between mucin and CS, modified CS (MA-CS, MBI-MA-CS). The mucin should be spontaneously adsorbed on the surface of the CS and modified CS. The mucoadhesive property of the chitosan and its derivatives was assessed by suspension of mucin in their aqueous solutions (in pH 1.2, 4.0 and 6.4) at room

temperature. The linearity range for mucin at the wavelength of detection at 555 nm was obtained as 0.1-0.5 mg/mL. The linear equations obtained by least square method were $y = 0.4957x - 0.001$, $y = 1.0897x - 0.0488$ and $y = 1.5004x + 0.245$ in pH 1.2, 4.0 and 6.4, respectively (Appendix A).

4.4.2 Adsorption of mucin on polymer

In general, bioadhesion applied to mucous membrane in GTT are continuously described as mucoadhesion. The mechanism of mucoadhesion is considered to divide in two steps: the contact stage and the consolidation stage between the mucus and polymer. In this work the PAS colorimetric method was used to designate the amount of free mucin and the amount of adsorbed mucin on the chitosan and modified derivative chitosan (TMC, GA-TMC and SA-GA-TMC).

Table 4.2 Comparison of chitosan and modified chitosan (TMC, GA-TMC and SA-GA-TMC) to mucoadhesive property

Batch	Absorbed of mucin	Absorbed of mucin	Absorbed of mucin
	At pH 1.2 (mg/mL) (\pm SD,n=3)	At pH 4.0 (mg/mL) (\pm SD,n=3)	At pH 6.4 (mg/mL) (\pm SD,n=3)
CS	0.02 \pm 0.01	0.05 \pm 0.00	0.04 \pm 0.01
TMC	0.08 \pm 0.00	0.08 \pm 0.01	0.08 \pm 0.02
GA-TMC	0.25 \pm 0.03	0.38 \pm 0.01	0.37 \pm 0.00
SA-GA-TMC	0.20 \pm 0.01	0.29 \pm 0.01	0.35 \pm 0.01

The amount of mucin that was adsorbed onto the polymer (SA-GA-TMC) decreased at low pH values, being maximal at pH 6.4 (SIF) and minimal at pH 1.2 (SGF) were summarized in Table 4.2 and Figure 4.7. At pH 1.2 (SGF) chitosan showed an adsorbed mucin about 0.02 mg/ml, while the TMC showed higher adsorption of mucoadhesion than that for chitosan. Resulting that, at pH 1.2 the amine ($-\text{NH}_2$) groups of chitosan were partially protonated to the ammonium cation ($-\text{NH}_3^+$) because pK_a of chitosan was 6.5-6.8. It was not completely interact with negative charge of native mucin ($\text{pK}_a = 2.6$). When the CS was formed to the TMC, the high degree of quaternization may be increased the mucoadhesive properties. Because of the positive charge increased, it can interaction with negative charge of native mucin increase in the mucoadhesive properties. In case of GA-TMC, it showed an adsorbed mucin about 0.25 mg/ml the mucoadhesive forces were likely to be forced by

electrostatic interactions and the -OH part of GA groups on the polymer residue that interact with the -CH₃ groups on the mucin side chains result in a absorbed mucin was increasingly. In case of SA- GA-TMC, it showed an adsorbed mucin about 0.20 mg/ml, it displayed lower adsorption of mucoadhesion than GA-TMC. It was explained by changes in the conformation of the respective SA-GA-TMC polymer due to high steric hindrance and insoluble water effect of the SA side chain which makes it difficult for the interact with the -CH₃ groups on the mucin side chains leading to decrease the mucoadhesiveness. At the pH 4.0, the mucoadhesive ability of CS, TMC, GA-TMC and SA-GA-TMC were higher mucoadhesive properties at pH 1.2 (SGF). However, the SA-GA-TMC displayed higher the absorption of mucoadhesion than CS about 5.82± 0.01 times. It was explained by pH 4.0, the partial amino groups of CS were protonated (-NH₃⁺), the ionization of sialic acid (COO⁻ groups) increased leading to the ionic interaction with CS. These results are also consistent with pH 1.2 that the mucoadhesiveness increased from CS to GA-TMC and from CS to SA-GA-TMC. Therefore, the effect of hydrophobic, hydrogen and electrostatic effects impact on the mucoadhesion of CS, TMC, GA-TMC and SA-GA-TMC.

In pH 6.4, the amino groups of CS was deprotonated. Therefore, the electrostatic interaction between the positive charges of the CS (-NH₃⁺ group) with COO⁻ groups on the mucin decreased. Furthermore, the mucoadhesiveness of SA-GA-TMC, the resulting of increment of mucoadhesiveness from CS because of the hydrogen and hydrophobic effects, -OH and -CH₃ side chain on polymer interact in

part with the - CH₃ groups on the mucin side chains. This result is the evidence for the absorbed mucin of SA-GA-TMC at pH 6.4 that the mucoadhesiveness increased from CS about 7.85±0.02 times. Therefore, the effect of electrostatic, hydrogen and hydrophobic effects impact on the mucoadhesion of CS, TMC, GA-TMC and SA-GATMC in higher pH range.

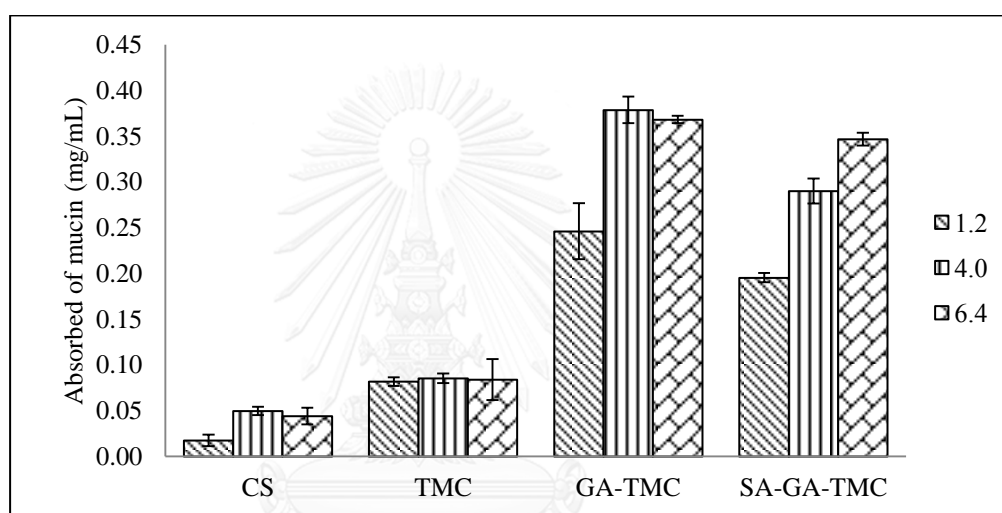


Figure 4.7 Adsorption of mucin on CS, TMC, GA-TMC and SA-GA-TMC at pH 1.2, 4.0 and 6.4. Data are shown as the mean \pm SD and derived from three independent repeats.

4.5 Morphology of SA-GA-TMC with SV encapsulation

The SA-GA-TMC micelle used in pharmaceutical dosage forms, particularly as a vehicle for controlled drug delivery. Figure 4.8 showed the morphology of the SV

loaded SA-GA-TMC micelles were of an acceptable spherical shape and micellar size decreased with increasing the charged amount of SV loading. This may due to the hydrophobic interaction between SV and SA was enhanced. This result is the evidence from the SEM images of 10% SV loaded SA-GA-TMC and 20% SV loaded SA-GA-TMC.

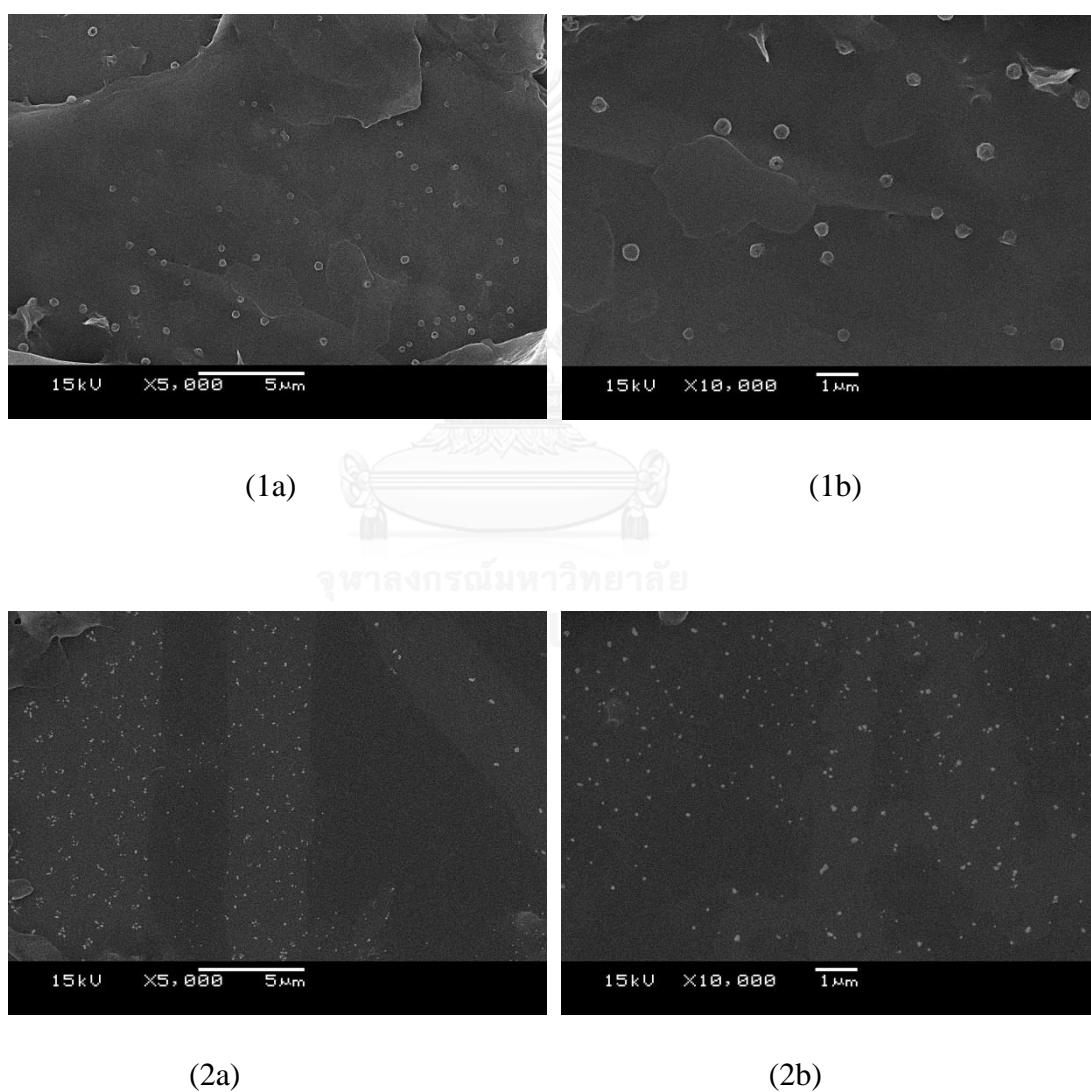


Figure 4.8 Representative SEM images of SA-GA-TM (1a-b) with 10% SV and SA-GA-TMC (2a-b) with 20% SV.

4.5.1 Particles size, size distribution

Size distribution and particle size of micelles (SA-GA-TMC) with and without SV loading were presented in Table 4.3.

From the Table 4.3, the size of micelles obtained from the determination of Zetasizer analyzer. In case of the size distributions of SA-GA-TMC with SV showed that they were in the range approximately from 182-301 nm with PDI from 0.13 to 0.34. Overall, the size after drug (10 and 20% of SV into SA-GA-TMC) loading was decreased compared with blank SA-GA-TMC micelles. The causes were mainly attributed to the mechanism of SA-GA-TMC micelle aggregation. The hydrophobic chain of stearic acid had weak hydrophobic interaction compared with other hydrophobic polymers. After SV loading, the cohesive force of the hydrophobic interaction was enhanced and thus caused the decrease of the size [57].

4.5.2 Zeta potential (Zp)

Zeta potential measurements will give information about the overall surface charge of the particles and how this is affected by changes in the environment [27]. When considering the zeta potential, that is surface charge, it can greatly influence particle stability in suspension through the electrostatic repulsion between particles.

The surface of CS was found to possess positive charge of 34.06 ± 1.70 mV and 39.93 ± 2.71 mV for TMC and 40.53 ± 0.58 for GA-TMC because the amount of positive charges on the polymer chain is increased. The surface positive charges of SA-GA-TMC micelles were increased 41.90 ± 1.32 mV. This may due to the micelles with SA had smaller micellar size, which might result from the increasing hydrophobic interaction among SA chain. The smaller size which meant larger surface area would have higher surface charge density and thus a higher surface zeta potential [58].

Zeta potential values are also of interest for the characterization of the SV loaded SA-GA-TMC micelles display Z_p values 46.03 ± 0.73 and 47.86 ± 0.75 mV (10% SV-SA-GA-TMC and 20% SV-SA-GA-TMC, respectively). After the SV loading, the zeta potential indicated no signal change.

Table 4.3 Properties of Synthesized chitosan micelles and Prepared SV Loaded SA-GA-TMC micelles

Abbreviations	Particle size*±SD (nm)	Zeta potential (mv)	CMC (µg / mL)	% EE	% DL	Polydispersity Index
SA-GA-TMC	1093 ± 4.73	41.90 ± 1.32	3.98	-	-	0.80 ± 0.04
10% SV-SA-GA-TMC	301 ± 2.83	46.03 ± 0.73	-	44.44 ± 1.02	4.00 ± 0.32	0.34 ± 0.01
20% SV-SA-GA-TMC	182 ± 1.57	47.86 ± 0.75	-	88.12 ± 0.75	14.10 ± 0.43	0.13 ± 0.03

Particle size* measured by Zetasizer analyzer. Data represent the mean (standard deviation (n = 3)).

4.5.3 Mucoadhesiveness of SA-GA-TMC with SV

Mucoadhesiveness of polymeric micelles was measured as a able to test their ability to bind to the mucosal surface of the mucin. The results of in vitro mucoadhesive of the spheres with mucin in three different buffers (pH 1.2, 4.0 and 6.4) are shown in Figure 4.8 by PAS method.

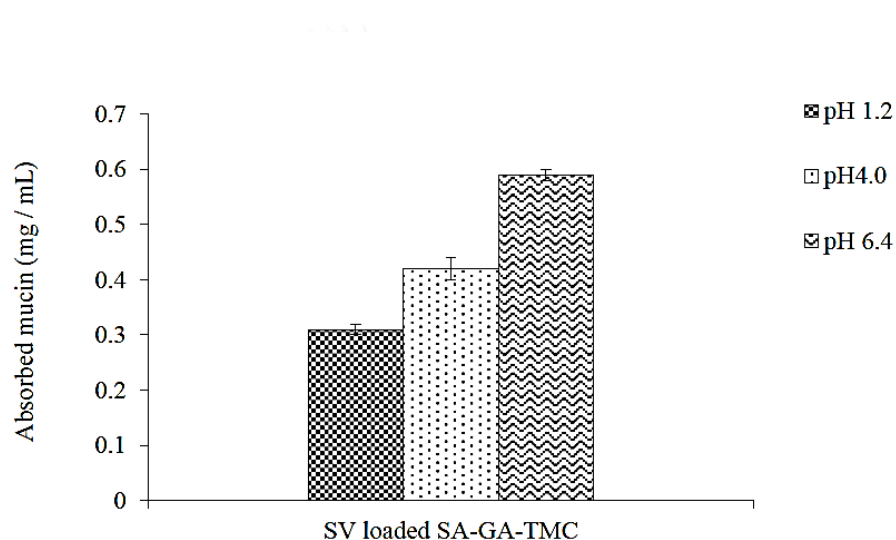


Figure 4.9 Adsorption of mucin on SA-GA-TMC micelles with 10% SV at pH 1.2, 4.0 and 6.4. Data are shown as the mean \pm SD.

According to the results, the mucoadhesive of SA-GA-TMC micelles with SV loading were exhibited excellent mucoadhesiveness with 1.35 ± 0.01 , 1.51 ± 0.02 and 1.68 ± 0.01 mg/mL at pH 1.2, 4.0 and 6.4, respectively higher than that SA-GA-TMC without SV at the same pH buffers. This result was the evidence from the electrostatic effects, indicating that after the SV loaded in SA-GA-TMC micelles, the

size of micelles decrease to be small micelles containing positive charge on the surface micelles lead to mucoadhesiveness higher than SA-GA-TMC without SV, which is likely to be due to the fact that the influence of the positive charge was enough to increase the mucoadhesion.

4.6 Characterization of SA-GA-TMC micelle with SV

4.6.1 Fourier transform infrared spectroscopy (FTIR)

FTIR spectroscopy was used to determine the chemical interaction between the drug and SA-GA-TMC, samples of 10% SV loaded SA-GA-TMC and 20% loaded SA-GA-TMC were investigated in Figure 4.10. The FTIR spectrum of SV (Figure. 4.10a) showed the -OH stretching absorption band at 3543 cm^{-1} . The absorption bands at 3014 , 2960 and 2829 cm^{-1} were attributed to the C-H stretching vibrations. The main characteristic peaks of SV at 1721 and 1640 cm^{-1} were due to the stretching bands of ester and lactone carbonyl group. The C-H in-plane bending vibration and skeletal C-C vibrations are observed in the region $1350\text{-}950\text{ cm}^{-1}$. The C-H out-of plane bending modes are usually of weak intensity arises in the region $900\text{-}600\text{ cm}^{-1}$ [33].

The FTIR spectrum of 10% and 20% SV loaded SA-GA-TMC. Figure 4.10b and 4.10c showed the characteristic peak at 2921 cm^{-1} and 1710 cm^{-1} corresponding to the C-H stretching vibration and ester stretching peaks of SV, respectively. The peak

at 1224 cm^{-1} was due to the C-H in-plane bending vibration. The peaks at 893, 797 and 655 cm^{-1} correspond to C-H in-plane bending vibrations of SV. These SV characteristic peaks were shifted in the formulations suggesting the interactions between SV and SA-GA-TMC. The FTIR spectrum appeared can be confirming the successful loading of SV on SA-GA-TMC micelles.

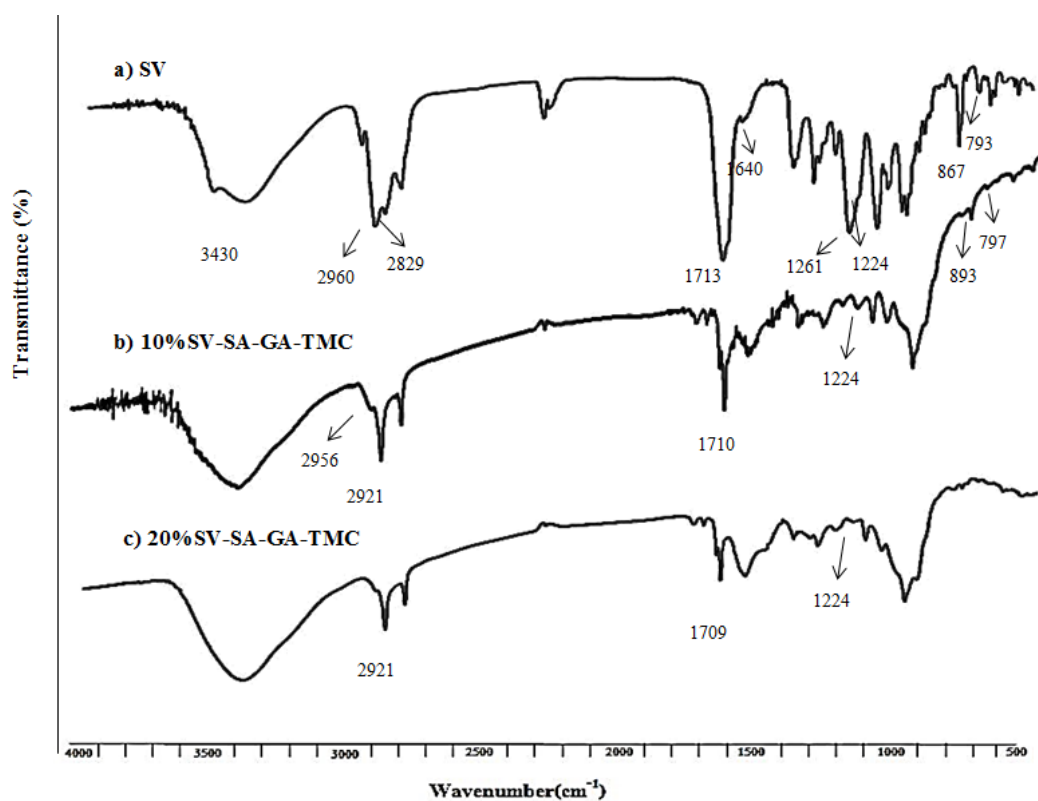


Figure 4.10 FTIR spectra of (a) SV, (b) 10% SV-SA-GA-TMC and (c) 20% SV-SA-GA-TMC micelles.

4.7 Evaluation of drug encapsulation and drug loading efficiency (%EE and %DL)

Simvastatin was physically consolidated within the hydrophobic cores of the micelles using dialysis method. The percentages of encapsulation efficiency (EE) and drug loading ratio (DL) of the SV loaded SA-GA-TMC micelles were shown in Table 5 that were analyzed by an Ultraviolet (UV) spectrophotometer at 238 nm with the linear equation $y = 0.0516x - 0.0036$ of the standard curve.

The encapsulation efficiency and drug loading ratio of 10 and 20% SV loaded SA-GA-TMC were $44.44 \pm 0.01\%$, $4.00 \pm 0.01\%$ and $88.12 \pm 0.02\%$, $14.10 \pm 0.01\%$, respectively (Table 4.3). After the SV loading, the size drug loading was decreased compared with SA-GA-TMC. This is due to the mechanism of SA-GA-TMC micelle aggregation. The hydrophobic chain of stearic acid had weak hydrophobic interaction compared with other hydrophobic polymers [59]. Then drug loading, the cohesive force of the hydrophobic interaction was improved and thus caused the decrease of size.

Table 4.4 Encapsulation and drug loading of SV loaded SA-GA-TMC

Formulations	% Encapsulation	% Drug loading
10%SV/SA-GA-TMC	44.44±0.01	4.00 ± 0.01
20%SV/SA-GA-TMC	88.12±0.02	14.10±0.01

4.8 In vitro release profiles

The releases of SV drug from SA-GA-TMC micelles were performed at a function of time in buffers pH 1.2, 4.0 and 6.4 (SGF, vaginal fluids and SIF, respectively) at 37 ± 1 °C. The linear equations of SV calibration curve obtained by the least square method being $y = 0.0277x + 0.0069$, $y = 0.0314x - 0.0038$ and $y = 0.0382x - 0.0041$ for the assay in pH 1.2, 4.0 and 6.4, respectively (Appendix B).

As a function of pH, presents the releasing profiles of SV from SA-GA-TMC in three different buffers (pH 1.2, 4.0 and 6.4) were shown on Figure 4.11.

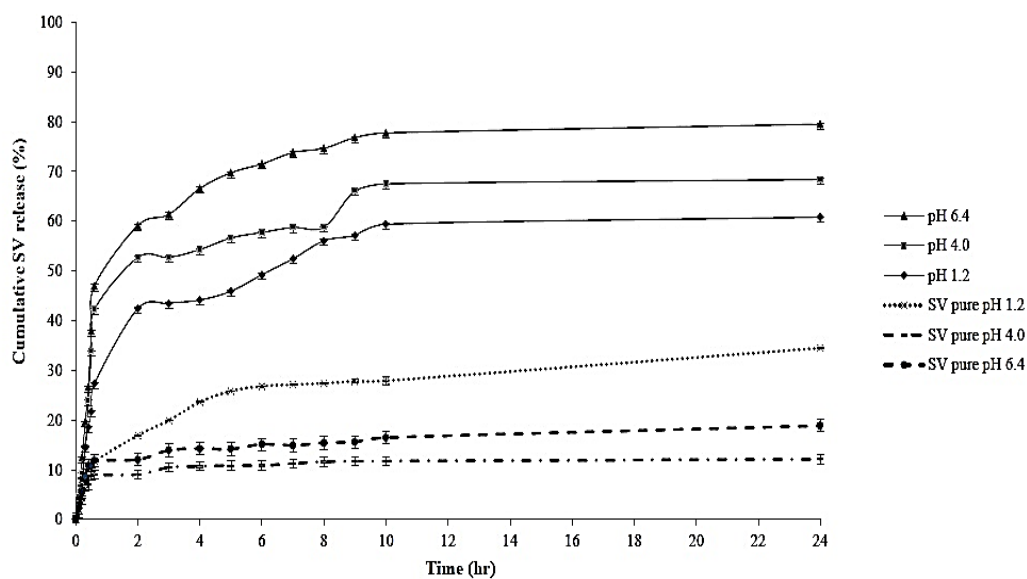


Figure 4.11 Release profiles of 10% simvastatin from SA-GA-TMC micelles in three different buffers, $37 \pm 1^\circ\text{C}$ (average \pm SD, $n=3$).

The release profiles of the 10% SV loaded SA-GA-TMC micelles showed the initial burst release in the early stage. The burst release (1 h) was due to the presence of more free drug on the micelle surface. The cumulative drug release percentages are approximately 60, 68 and 79% within 24 h in pH 1.2, 4.0 and 6.4 respectively. Moreover, the most release behavior of SV in pH 6.4 from SA-GA-TMC micelles was more than that pH 1.2 and 4.0. The results were due to effect of the increasing size of the micelles in pH 6.4 (376 nm). Compared to size of micelles in pH 1.2 and 4.0 are 344 and 362 nm, respectively within 24 h.

According to the results, we found that the cumulative drug release profiles of SV loaded SA-GA-TMC micelles were suitable for sustained release of SV than

pure SV because the SA-GA-TMC micelles could prolonged release of SV for the all three tested pH within the first 4 h up to 66% and SV was still sustained release within 24 h in pH 6.4.

The vitro release profiles of 10 and 20% SV loaded SA-GA-TMC micelles were investigated in pH 1.2, 4.0 and 6.4 for 24 h (Figure 4.12 – 4.14).

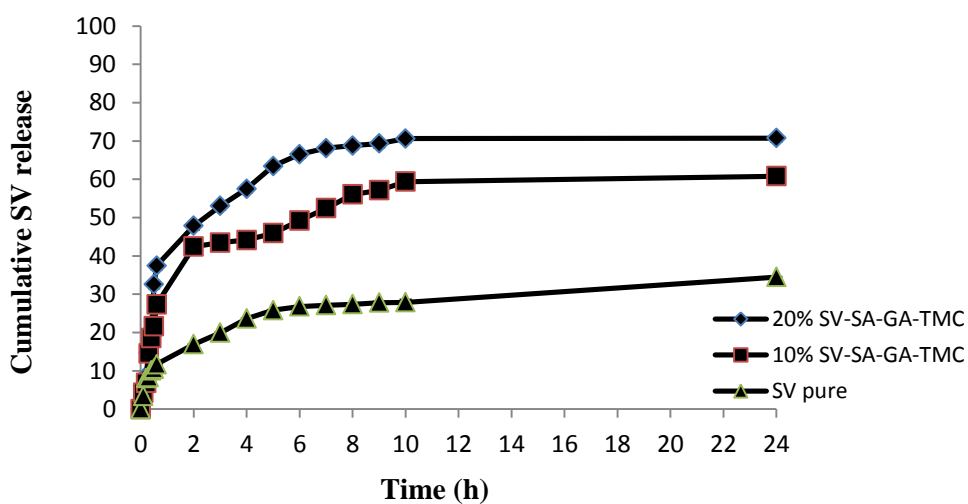


Figure 4.12 Release profiles of 10% and 20% simvastatin from SA-GA-TMC micelles in pH 1.2 buffers, 37 ± 1 °C (average \pm SD, n=3).

The cumulative release of SV showed that the SA-GA-TMC micelles can be prolonged release of SV within the 24 h. The release profiles of the 20% SV loaded SA-GA-TMC show the initial burst release in first stage (1 h) with higher than of 10% SV loaded SA-GA-TMC micelles. The burst release was considered to be due to the

presence of more free drugs on the surface of micelles. Moreover, about 50% SV was released in 3 h and 7 h for 20% SV loaded SA-GA-TMC and 10% SV loaded SA-GA-TMC micelles, respectively and still sustained release within 24 h. The tendency of cumulative release from 10% and 20% SV loaded SA-GA-TMC micelles at pH 4.0 and 6.4 is similar pH 1.2 (Figure 4.13 – 4.14).

Overall, from these results indicated that SV loaded SA-GA-TMC micelles released the drug increasingly and sustainable release than pure SV.

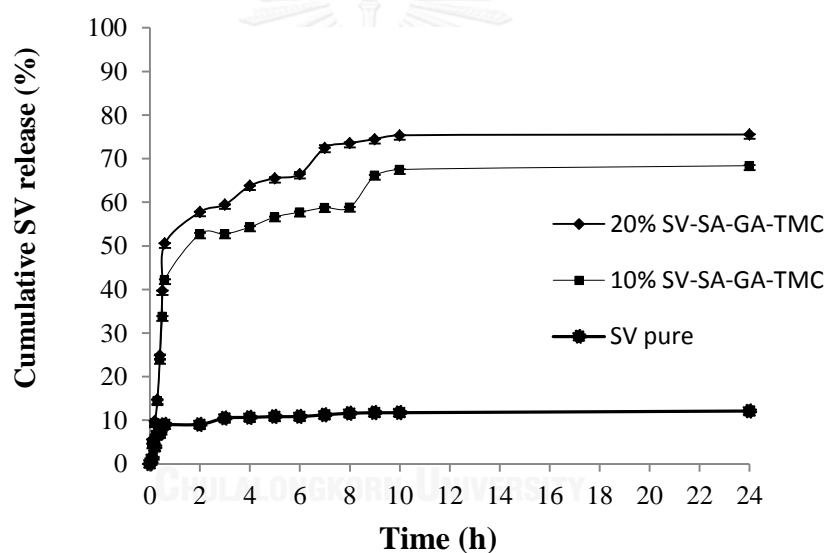


Figure 4.13 Release profiles of 10% and 20% simvastatin from SA-GA-TMC micelles in pH 4.0 buffers, $37 \pm 1^\circ\text{C}$ (average \pm SD, n=3).

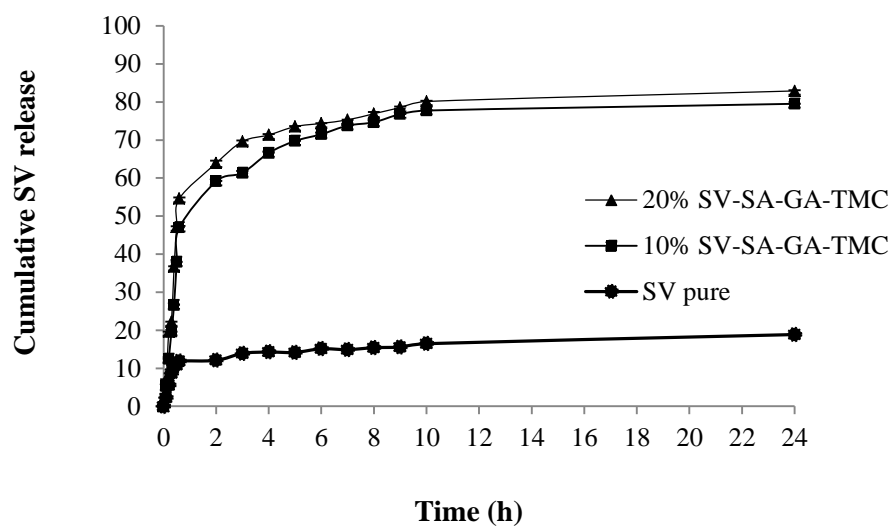
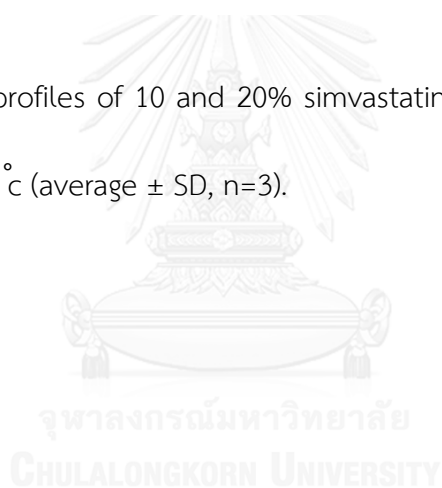


Figure 4.14 Release profiles of 10 and 20% simvastatin from SA-GA-TMC micelles in pH 6.4 buffers, 37 ± 1 °C (average \pm SD, n=3).



CHAPTER V

CONCLUSION AND SUGGESTION

5.1 Conclusion

In this study, the SA-GA-TMC was synthesized to form micelle by self-assembly with a CMC of 3.98 $\mu\text{g}/\text{mL}$. The first step, the reaction of CS to form *N*-trimethylchitosan by methyl iodide was attacked with the amino groups of CS and then the GA and SA were covalently reacted at the amino groups of CS using EDAc as activator. The degree of quaternization (%DQ) of chitosan and the degree of substitution (%DS) of gallic acid and stearic acid were calculated by ^1H NMR about 24.33 ± 0.18 (%DQ) and 5.00 ± 0.02 (%DS) and 21.77 ± 0.07 (%DS), respectively.

The Perriodic acid: Schiff (PAS) colorimetric method was used to designate the amount of free mucin and the amount of adsorbed mucin on the chitosan and modified derivative chitosan in the simulated gastrointestinal fluid (pH 1.2, 4.0 and 6.4). The data suggests that the lowest pH (1.2) SA-GA-TMC shows the highest mucoadhesive property.

The characterizations of SA-GA-TMC appear to be promising polymer for the development of various drug delivery carries at mucus sites. Simvastatin (SV) was successfully loaded into SA-GA-TMC micelles by dialysis method. The morphology of SA-GA-TMC with and without SV was obtained by SEM, showed a good spherical

shape with SV loaded into SA-GA-TMC micelles. The encapsulation of 10% SV loaded SA-GA-TMC micelles showed 44.44%. Moreover, increasing of SV loaded from 10 to 20 %SV-SA-GA-TMC (w/w) micelles found that increased 44.44 to 88.12% drug entrapment. The SV loaded SA-GA-TMC micelles can be prolonged and sustained release profiles of SV within 24 h.

Mucoadhesiveness of SA-GA-TMC micelle with SV was showed 1.35 ± 0.01 , 1.51 ± 0.02 and 1.68 ± 0.01 mg/mL at pH 1.2, 4.0 and 6.4, respectively. Hence, the advantages of the controlled release system based on the mucoadhesive polymer can be improving by using the SA-GA-TMC micelles.

5.2 Suggest

The problem of simvastatin was the poorly absorbed from the gastrointestinal tract with less than 5%.

We are interested in studying the potent ability of the SA-GA-TMC in improving the bioavailability, maintaining higher concentration of the drug and prolonging circulation time in the intestinal tract. The intestinal absorption mechanism should be investigated.

REFERENCES

1. Laufs, U., Liao, J.K., Direct vascular effects of HMG-CoA reductase inhibitors. *Trends in Cardiovascular Medicine*, 2000(4): 143-148.
2. Carlucci, G., Mazzeo, P., Biordis, L., Bologna, M., Simultaneous determination of simvastatin and its hydroxy acid form in human plasma by high performance liquid chromatography with UV detection. *Journal of Pharmaceutical & Biomedical Analysis*, 1992(9): 693-699.
3. Margulis-Goshen, K., Magdassi, S., Formation of simvastatin nanoparticles from microemulsion. *Nanomedicine*, 2009(3): 274-281.
4. Tiwari, R., Pathak, K., Nanostructured lipid carrier versus solid lipid nanoparticles of simvastatin: Comparative analysis of characteristics, pharmacokinetics and tissue uptake. *International Journal of Pharmaceutics*, 2011(7): 55-62.
5. Jadhav, S., Jain, G., Statins and osteoporosis: new role for old drugs. *Journal of Pharmacology and Pharmacotherapeutics*, 2006(1): 3-18.
6. Park, J., The use of simvastatin in bone regeneration, *Med. Oral Patol Oral Cir Bucal*, 2009(9): 485-488.
7. Xiangning, L., Xiaoran, L., Lei, Z., Effects of simvastatin-loaded polymeric micelles on human osteoblast-like MG-63 cells. *Colloids and Surfaces B: Biointerfaces*, 2013(1): 420-427.

8. Jaime, G., Isabel, S., Angel, C., Carmen, A., Interactions at the Air–Water Interface and in Bulk Solution. *The Journal of Physical Chemistry C*, 2010(2): 1181-1189.
9. Mishra, S., Kumar, G., Kothiyal, P., Formulation and Evaluation of Buccal Patches of Simvastatin by Using Different Polymers. *The Pharma innovation*, 2012(1): 87-92.
10. Hägerström, H., Edsman, K., Strømme, M., Low- Frequency Dielectric Spectroscopy as a Tool for Studying the Compatibility between Pharmaceutical Gels and Mucus Tissue. *Journal of Pharmaceutical Sciences*, 2003(9): 1869-1881.
11. Bernkorp-Schnurch, A., Kast, C.E., Guggie, D., Permeation enhanceing polymer in oral delivery of hydrophilic macromolecule: thiomers/GSH system. *Journal of Controlled Release*, 2003(1): 95-103.
12. Patil, S.B., Murthy, R.S., Mahajan, H.S., Mucoadhesive polymers: Means of improving drug delivery. *International Journal of Pharmaceutics* 2007(38): 102-109.
13. Tilloo, S.K., Rasala, T.M., Kale, V., Mucoadhesive microparticulate drug delivery system. *International Journal of Pharmaceutical Sciences Review and Research*, 2011(9): 52-56.

14. Michael, L., Joke, A., Etienne, H., In vitro evaluation of mucoadhesive properties of chitosan and some other natural polymers. *International Journal of Pharmaceutics*, 1992(1): 43-48.
15. Mythri, G.K., Kavith, M., Rupesh Kumar, Sd., Novel Mucoadhesive Polymers –A Review. *Journal of Applied Pharmaceutical Science*, 2011(1): 37-42.
16. Mao, S., Sun, W., Kissel, T., Chitosan-based formulations for delivery of DNA and siRNA. *Advanced Drug Delivery Reviews*, 2010(1): 12-27.
17. Dodane, V., Vilivalam, V., Pharmaceutical applications of chitosan- A Review. *International Journal of Pharmaceutics* 1998(1): 246-251.
18. Trickler, W., Nagvekar, A., Dash, A., A novel nanoparticle formulation for sustained paclitaxel delivery. *AAPS PharmSciTech*, 2008(2): 486-93.
19. Park, J., Saravanakumar, G., Kim, K., Targeted delivery of low molecular drugs using chitosan and its derivatives. *Advanced Drug Delivery Reviews*, 2010(1): 28-41.
20. Kotze, A.F., Thanou, M.M, Lueben, H.L., Enhancement of Paracellular drug transport with highly quaternized N-trimethyl chitosan chloride in neutral environments: in vitro evaluation in intestinal epithelial cell (Caco-2). *Journal of Pharmaceutical Sciences*, 1999(2): 253-257.
21. Hamman, J.H., Stander, M., Junginger, H.E., Enhancement of paracellular drug transport across mucosal epithelia by N-trimethyl chitosan chloride. *STP Pharma Sciences*, 2000(1): 35-38.

22. Thanou, M.M., Kotze, A.F, Scharringhausen, T., Effect of degree of quaternization of N-trimethyl chitosan chloride for enhanced transport of hydrophilic compounds across intestinal Caco-2 cell monolayers. *Journal of Controlled Release*, 2000(1): 15-25.
23. Kotze, A.F., Thanou, M.M., Lueben, H.L., Effect of degree of quaternization of N-trimethyl chitosan chloride on the permeability of intestinal epithelia cell (Caco-2). *European Journal of Pharmaceutics and Biopharmaceutics*, 1999(72): 269-274.
24. Dewald, S., Josias, H.H, Awie, F.K., Evaluation of the Mucoadhesive Properties of N-Trimethyl Chitosan Chloride. *Drug Development and Industrial Pharmacy*, 2003(1): 61-69.
25. Duhem, N., Rolland, J., Riva, R., Tocol modified glycol chitosan for the oral delivery of poorly soluble drugs. *International Journal of Pharmaceutics*, 2011(2): 452-460.
26. Li, H., Huo, M., Zhou, J., Enhanced oral absorption of paclitaxel in N-deoxycholic acid-N, O-hydroxyethyl chitosan micellar system. *Journal of Pharmaceutical Sciences*, 2010(11): 4543-4553.
27. Mo, R., Xiao, Y., Sun, M., Enhancing effect of N-octyl-O-sulfate chitosan on etoposide absorption. *International Journal of Pharmaceutics*, 2011(1-2): 38-45.

28. Yuan, H., Lu, L., Du, Y., Stearic acid-g-chitosan polymeric micelle for oral drug delivery: in vitro transport and in vivo absorption. *Molecular Pharmaceutics*, 2011(1): 225-38.
29. Zhenshan, J., Yijia, Z., Yen, H., Simvastatin prodrug micelles target fracture and improve healing. *Journal of Controlled Release*, 2015(10): 23–34.
30. Hu, F.Q., Zhao, M.D., Yuan, H., You, J., Du, Y.Z., Zeng, S., A novel chitosan oligosaccharide–stearic acid micelles for gene delivery: properties and in vitro transfection studies. *International Journal of Pharmaceutics*, 2006(1-2): 158–166.
31. Shi, B., Fang, C., Stealth MePEG-PCL micelles: effects of polymer composition on micelle physicochemical characteristics, in vitro drug release, in vivo pharmacokinetics in rats and biodistribution in S180 tumor bearing mice. *Colloid and Polymer Science* 2005(9): 954–967.
32. Kohori, F., Yokoyama, M., Sakai, K., Process design for efficient and controlled drug incorporation into polymeric micelle carrier systems. *Journal of Controlled Release*, 2002(1): 155-163.
33. Ungaro, F., Giovino, C., Use of cyclodextrins as solubilizing agents for simvastatin: Effect of hydroxypropyl- β -cyclodextrin on lactone/hydroxyacid aqueous equilibrium. *International Journal of Pharmaceutics*, 2011(1): 49–56.
34. Uhrich, K.E., Cannizzaro, S. M., Langer, R. S., Polymeric Systems for Controlled Drug Release. *Chemical Reviews*, 1999(11): 3181-3198.

35. Ganji, F., Hydrogels in Controlled Drug Delivery Systems. Iranian Polymer Journal 2009(1): 63-88.
36. Leong, K.W., Langer, R., Polymeric controlled drug delivery. Advanced Drug Delivery Reviews, 1988(1): 199-233.
37. Tilloo, S.K., Rasala, T. M., Kale, V.V., Mucoadhesive microparticulate drug delivery system. Journal of Pharmaceutics and Biopharmaceutics, 2011(9): 52-56.
38. Mythri, G.K., Kavitha, M., Novel mucoadhesive polymer- A Review. Journal of Applied Pharmaceutical Science 2011(8): 37-42.
39. Smart, J.D., The basics and underlying mechanisms of mucoadhesion. Advanced Drug Delivery Reviews 2005(11): 1556-1568.
40. PrasadRao, J., Kurte, G., Polymer nanoparticles: Preparation techniques and size control parameters, Progress in Polymer Science G Model. Journal of Pharmaceutical Sciences 2011: 674.
41. Fessi, H., Puisieux, F., Devissaguet, J., Nanocapsule formation by interfacial deposition following solvent displacement. International Journal of Pharmaceutics, 1989(1): R1- R4.
42. Kostog, M., Kohler, S., Liebert, T., Pure cellulose nanoparticles from trimethylsilylcellulose. Macromolecular Symposia, 2010(2): 96-106.

43. Jeon, H., Jeong, Y., Jang, M., Effect of solvent on the preparation of surfactant free poly(*dl*-lactide-co-glycolide) nanoparticles and norfloxacin release characteristics. *International Journal of Pharmaceutics*, 2000(1-2): 99–108.
44. Jeong, Y., Cho, C., Kim, S., Preparation of poly(*dl*-lactide- co-glycolide) nanoparticles without surfactant. *Journal of Applied Polymer Science*, 2001(12): 2228–22236.
45. Sajomsang, W., Gonil, P., Synthesis and antibacterial activity of methylated N-(4-N,N-dimethylaminocinnamyl) chitosan chloride. *European Polymer Journal*, 2009(8): 2319-2328.
46. Anupama, S., Arun, K.G., Surface modified dendrimers: Synthesis and characterization for cancer targeted drug delivery. *Bioorganic & Medicinal Chemistry*, 2011(11): 3341-3346.
47. Kilcoyne, M., Gerlach, J.Q., Periodic acid–Schiff’s reagent assay for carbohydrates in a microtiter plate format. *Analytical Biochemistry* 2011(1): 18–26.
48. Alessandro, F.M., Antonio, G.B., Characterization of polyelectrolytes complex based on N,N,N-trimethyl chitosan/heparin prepared at different pH conditions. *Carbohydrate Polymers*, 2011(2): 1266– 1272.
49. Hamman, H.J., Kotze, F.A., Effect of the type of base and number of reaction steps on the degree of quaternization and molecular weight of N- trimethyl

- chitosan chloride. *Drug Development and Industrial Pharmacy*, 2001(1): 373-380.
50. Moury, K.V., Nazma, N.I., Trimethyl chitosan and its applications in drug delivery. *Journal of Materials Science. Materials in medicine*, 2009(5): 1057-1079.
51. Myung-Kwan, C., Chong-Su, C., Hoo-Kyun, C., Mucoadhesive drug carrier based on interpolymer complex of poly(vinyl pyrrolidone) and poly(acrylic acid) prepared by template polymerization. *Journal of Controlled Release*, 2002(3): 327-334.
52. Park, J.S., Akiyama, Y., Yamasaki, Y., Preparation and characterization of polyion complex micelles with a novel thermosensitive poly(2-isopropyl-2-oxazoline) shell via the complexation of oppositely charged block ionomers. *Langmuir*, 2007(1): 138-146
53. Kranbuehl, D.E., Verdier, P.H., Polymer Chains with Excluded Volume on a Cubic Lattice. Local Overlap Model. *Polymer Journal*, 1996(28): 543-547.
54. Can, Z., Ping, Q., Hongjuan Z., Self-assembly and characterization of paclitaxel-loaded N-octyl-O-sulfate chitosan micelles system. *Colloids and Surfaces B: Biointerfaces*, 2004(1): 69-75.
55. Anitha, A., Deepa, N., Chennazhi, K.P., Development of mucoadhesive thiolated chitosan nanoparticles for biomedical applications. *Carbohydrate Polymers*, 2011(1): 66-73.

56. Majeti, N.V., Kumar, R., A review of chitin and chitosan applications. *Reactive & Functional Polymers*, 2000(1): 1-27.
57. Hu, F.Q., Wu, X.L., Du, Y.Z., You, J., Yuan, H., Cellular uptake and cytotoxicity of shell cross-linked stearic acid-grafted chitosan oligosaccharide micelles encapsulating doxorubicin. *European Journal of Pharmaceutics and Biopharmaceutics*, 2008(1): 117–125.
58. Paruchuri, V.K., Nguyen, A.V., Miller, J.D., Zeta-potentials of self assembled surface micelles of ionic surfactants adsorbed at hydrophobic graphite surfaces. *Colloids Surface, A*, 2004(1): 519–526.
59. Hong, Y., Lin, J.L., Yong, Z.D. , Stearic Acid-g-chitosan Polymeric Micelle for Oral Drug Delivery: In Vitro Transport and in Vivo Absorption. *Molecular Pharmaceutics*, 2010(1): 225-238.



APPENDIX

จุฬาลงกรณ์มหาวิทยาลัย
CHULALONGKORN UNIVERSITY



APPENDIX A

Calibration curve of mucin (type II)

จุฬาลงกรณ์มหาวิทยาลัย
CHULALONGKORN UNIVERSITY

The concentration versus peak absorbance mucin glycoprotein (type II) determined by UV as the same condition described in chapter III is presented in Table 1A. The plot of calibration curve of mucin is illustrated in Figure 1A-3A.

Table 1A Absorbance of various concentrations of mucin (type II) at pH 1.2, 4.0 and 6.4 UV spectrophotomer

Concentration (mg/mL)	Absorbance		
	HCl (pH 1.2)	Acetate buffer (pH 4.0)	PBS (pH 6.4)
0.4	0.200	0.401	0.271
0.6	0.297	0.586	0.436
0.8	0.389	0.805	0.643
1.0	0.494	1.077	0.740
1.2	0.597	1.245	0.947

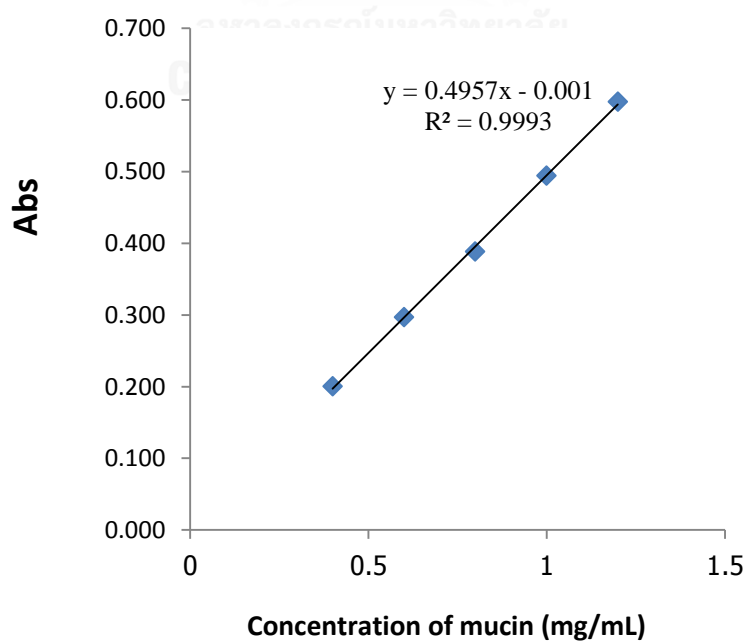


Figure 1A Standard curve of mucin at pH 1.2.

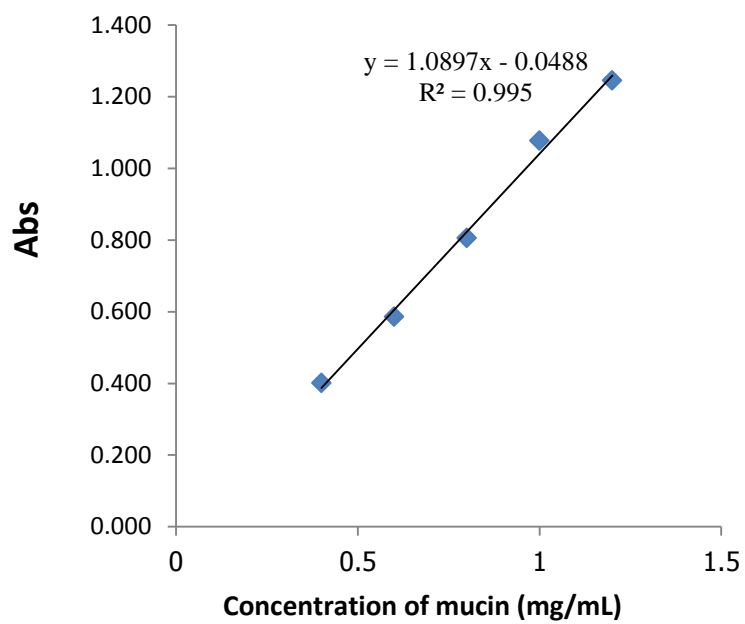


Figure 2A Standard curve of mucin at pH 4.0.

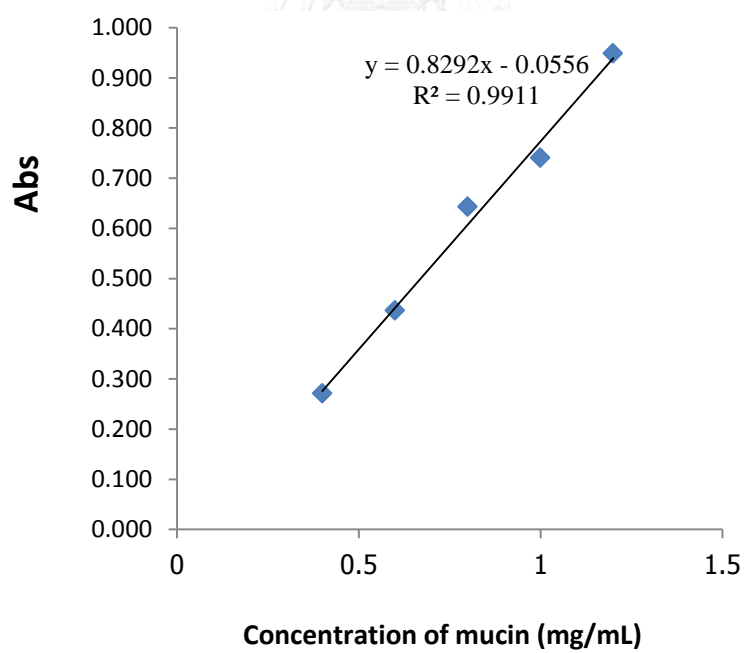


Figure 3A Standard curve of mucin at pH 6.4

Table 2A Absorbance of free and adsorbed mucin CS, TMC, GA-TMC and SA-GA-TMC in pH 1.2 by UV spectrophotometer.

Sample	Abs1	Abs2	Abs3	Adsorbed of mucin (mg/ml)	SD
Blank	0.128	0.104	0.103	$(1-x)/2$	
CS	0.582	0.591	0.594	0.02	0.01
TMC	0.529	0.527	0.520	0.082	0.00
GA	0.174	0.163	0.164	0.44	0.01
GA-TMC	0.331	0.392	0.364	0.25	0.03
SA-GA-TMC	0.408	0.412	0.418	0.20	0.01

Table 3A Absorbance of free and adsorbed mucin CS, TMC, GA-TMC and SA-GA-TMC in pH 4.0 by UV spectrophotometer.

Sample	Abs1	Abs2	Abs3	Adsorbed of mucin (mg/ml)	SD
Blank	0.297	0.340	0.272	$(1-x)/2$	
CS	1.231	1.235	1.240	0.05	0.00
TMC	1.152	1.162	1.160	0.085	0.01
GA	0.388	0.386	0.399	0.44	0.01
GA-TMC	0.509	0.535	0.511	0.38	0.01
SA-GA-TMC	0.696	0.722	0.716	0.29	0.01

Table 4A Absorbance of free and adsorbed mucin CS, TMC, GA-TMC and SA-GA-TMC in pH 6.4 by UV spectrophotometer.

Sample	Abs1	Abs2	Abs3	Adsorbed of mucin (mg/ml)	SD
Blank	0.199	0.178	0.180	$(1-x)/2$	
CS	0.876	0.888	0.894	0.04	0.01
TMC	0.824	0.796	0.840	0.084	0.02
GA	0.352	0.352	0.354	0.37	0.00
GA-TMC	0.351	0.351	0.344	0.37	0.00
SA-GA-TMC	0.379	0.381	0.392	0.35	0.01

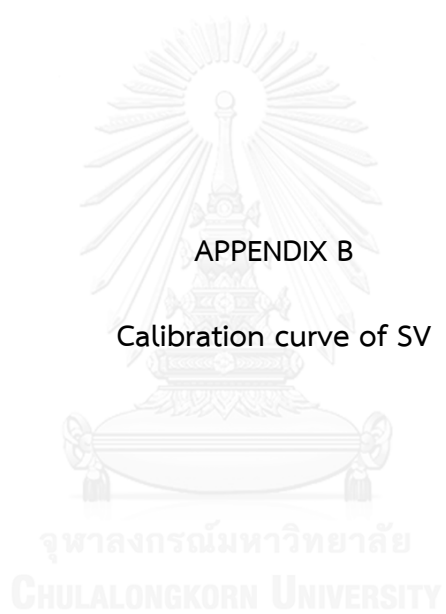


Table 1B Absorbance of simvastatin drug in 80% (v/v) EtOH determined in 238 nm

Concentration (ppm)	Abs	Abs	Abs	AVG	SD
3	0.164	0.164	0.164	0.164	0.000
6	0.311	0.312	0.311	0.311	0.000
9	0.457	0.458	0.458	0.458	0.001
12	0.592	0.592	0.593	0.593	0.000
15	0.765	0.765	0.766	0.765	0.000
18	0.907	0.907	0.908	0.907	0.000
21	1.107	1.108	1.109	1.108	0.001

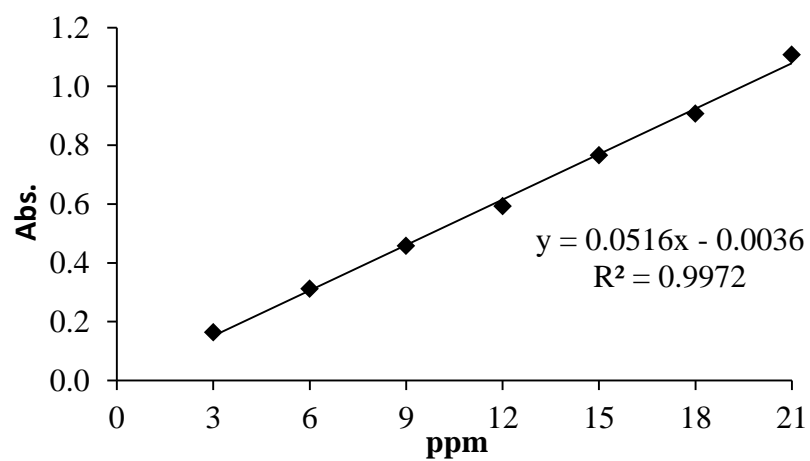
**Figure 1B** Calibration curve of simvastatin in 80% (v/v) EtOH determined in 238 nm.

Table 2B Absorbance of simvastatin drug in pH 1.2 determined in 238 nm

Concentration (ppm)	Abs	Abs	Abs	AVG	SD
6	0.165	0.165	0.165	0.165	0.000
9	0.273	0.273	0.273	0.273	0.000
12	0.334	0.333	0.335	0.334	0.001
15	0.423	0.423	0.425	0.423	0.001
18	0.505	0.505	0.505	0.505	0.000
21	0.591	0.591	0.591	0.591	0.000
24	0.657	0.657	0.658	0.657	0.000
27	0.747	0.747	0.747	0.747	0.000
30	0.852	0.852	0.852	0.852	0.000
33	0.921	0.921	0.921	0.921	0.000

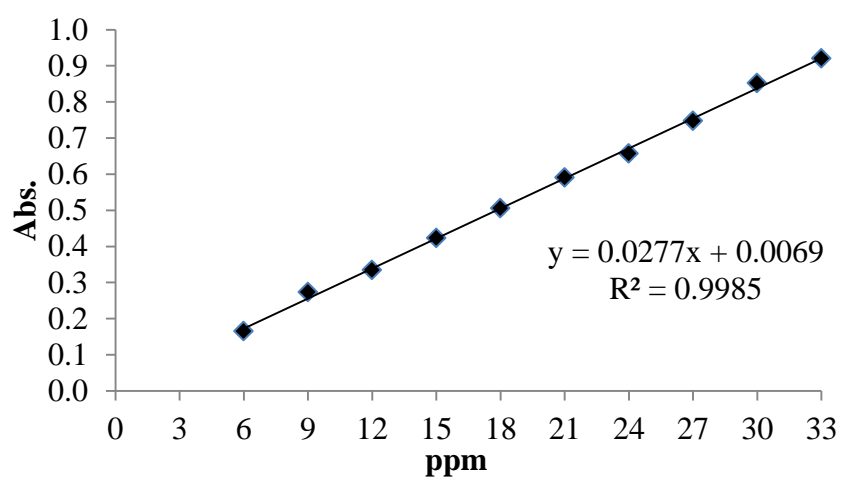


Figure 2B Calibration curve of simvastatin in pH 1.2 determined in 238 nm.

Table 3B Absorbance of simvastatin drug in pH 4.0 determined in 238 nm

Concentration (ppm)	Abs	Abs	Abs	AVG	SD
6	0.186	0.185	0.186	0.186	0.000
9	0.276	0.276	0.276	0.276	0.000
12	0.374	0.376	0.375	0.375	0.001
15	0.465	0.465	0.465	0.465	0.000
18	0.571	0.570	0.570	0.570	0.000
21	0.658	0.659	0.658	0.658	0.000
24	0.748	0.748	0.748	0.748	0.000
27	0.824	0.824	0.824	0.824	0.000
30	0.955	0.954	0.953	0.954	0.001

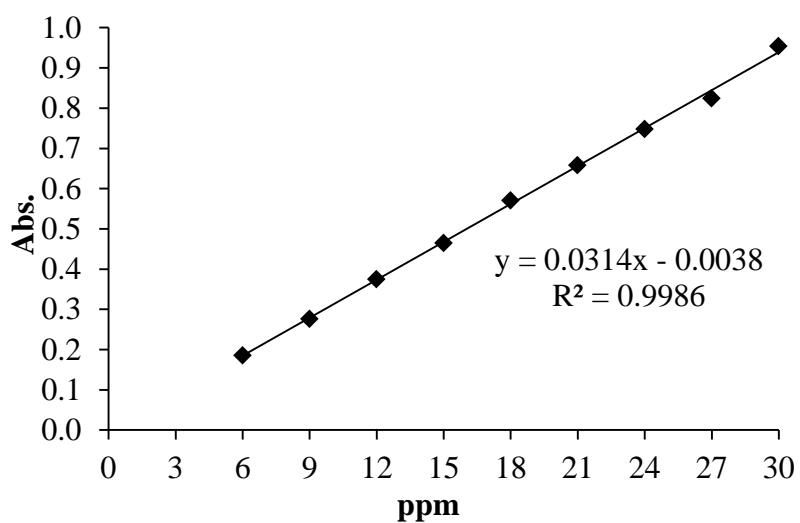


Figure 3B Calibration curve of simvastatin in pH 4.0 determined in 238 nm.

Table 4B Absorbance of simvastatin drug in pH 6.4 determined in 238 nm

Concentration (ppm)	Abs	Abs	Abs	AVG	SD
6	0.230	0.230	0.230	0.230	0.000
9	0.342	0.343	0.343	0.343	0.001
12	0.454	0.453	0.453	0.453	0.000
15	0.575	0.573	0.576	0.574	0.002
18	0.660	0.659	0.658	0.659	0.001
21	0.793	0.793	0.792	0.793	0.000
24	0.922	0.922	0.921	0.922	0.001
27	1.032	1.033	1.034	1.033	0.001

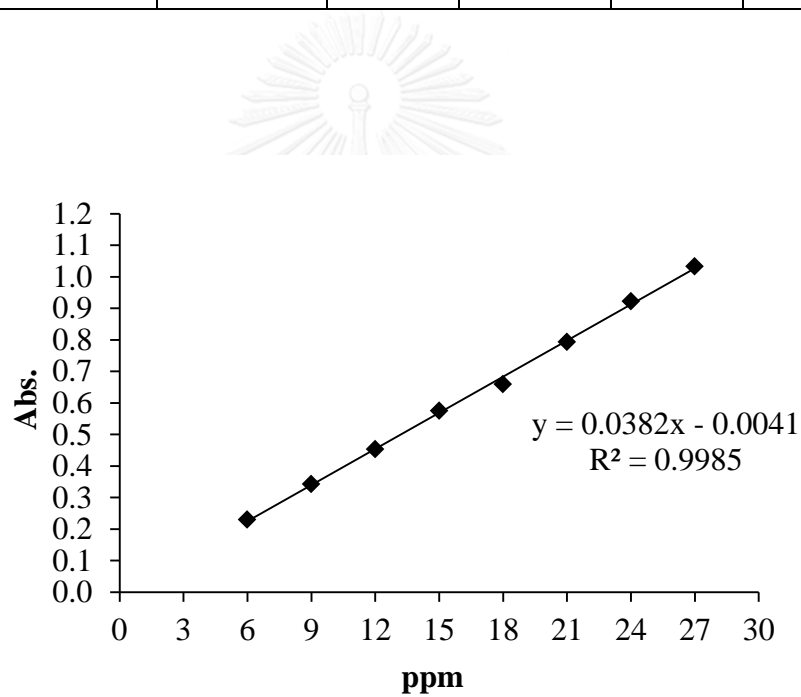


Figure 4B Calibration curve of simvastatin in pH 6.4 determined in 238 nm.



APPENDIX C

Encapsulation and Cumulative Drug Release

จุฬาลงกรณ์มหาวิทยาลัย
CHULALONGKORN UNIVERSITY

Table 1C Cumulative SV release from SA-GA-TMC micelles in pH 1.2

Time (min)	Abs.			Amount				
	Con 1	Con 2	Con 3	1	2	3	Mean	SD
0	0	0	0	0	0	0	0.000	0.000
10	0.15235	0.14989	0.15989	4.190	4.122	4.398	4.237	0.143
20	0.24630	0.25044	0.24989	6.774	6.888	6.873	6.845	0.062
30	0.53250	0.52190	0.53164	14.645	14.354	14.621	14.540	0.162
40	0.67690	0.66984	0.67541	18.617	18.423	18.576	18.538	0.102
50	0.79363	0.78531	0.78413	21.827	21.598	21.566	21.664	0.142
60	0.99415	0.98913	0.99740	27.342	27.204	27.431	27.326	0.115
120	1.54729	1.54368	1.53809	42.555	42.456	42.302	42.437	0.128
180	1.57953	1.58975	1.57267	43.441	43.722	43.253	43.472	0.236
240	1.60531	1.60469	1.60581	44.150	44.133	44.164	44.149	0.015
300	1.66498	1.67123	1.67245	45.792	45.963	45.997	45.917	0.110
360	1.78123	1.79394	1.79718	48.989	49.338	49.428	49.251	0.232
420	1.90314	1.91201	1.90597	52.341	52.586	52.419	52.449	0.125
480	2.04874	2.03253	2.03303	56.346	55.900	55.914	56.053	0.253
540	2.08022	2.06560	2.08567	57.212	56.810	57.362	57.128	0.285
600	2.16350	2.15432	2.15958	59.502	59.250	59.394	59.382	0.127
1440	2.21119	2.20935	2.21235	60.814	60.763	60.846	60.808	0.042

Table 2C Cumulative SV release from SA-GA-TMC micelles in pH 4.0

Time (min)	Abs.			Amount				
	Con 1	Con 2	Con 3	1	2	3	Mean	SD
0	0	0	0	0	0	0	0	0
10	0.16370	0.16496	0.17119	4.502	4.537	4.708	4.582	0.110
20	0.34398	0.34131	0.33982	9.460	9.387	9.346	9.398	0.058
30	0.52535	0.52258	0.53010	14.449	14.372	14.579	14.467	0.105
40	0.87136	0.87353	0.86931	23.965	24.024	23.908	23.966	0.058
50	1.23052	1.22353	1.23132	33.843	33.651	33.865	33.786	0.118
60	1.53982	1.53105	1.53622	42.349	42.108	42.250	42.236	0.121
120	1.91366	1.92806	1.90834	52.631	53.027	52.485	52.714	0.281
180	1.91529	1.91223	1.92283	52.676	52.592	52.883	52.717	0.150
240	1.96920	1.98239	1.97261	54.159	54.521	54.252	54.311	0.188
300	2.05822	2.06360	2.05376	56.607	56.755	56.484	56.615	0.136
360	2.09500	2.09726	2.10481	57.618	57.680	57.888	57.729	0.141
420	2.13105	2.13239	2.14312	58.610	58.647	58.942	58.733	0.182
480	2.14334	2.13748	2.13424	58.948	58.787	58.697	58.811	0.127
540	2.41038	2.40137	2.40150	66.292	66.044	66.048	66.128	0.142
600	2.45637	2.45385	2.45306	67.557	67.488	67.466	67.503	0.048
1440	2.48363	2.48155	2.49430	68.307	68.249	68.600	68.385	0.188

Table 3C Cumulative SV release from SA-GA-TMC micelles in pH 6.4

Time (min)	Abs.			Amount				
	Con 1	Con 2	Con 3	1	2	3	Mean	SD
0	0	0	0	0	0	0	0	0
10	0.19354	0.19314	0.19344	5.323	5.312	5.320	5.318	0.006
20	0.45393	0.45183	0.45392	12.484	12.427	12.484	12.465	0.033
30	0.71352	0.71180	0.71279	19.624	19.576	19.604	19.601	0.024
40	0.97354	0.96283	0.96739	26.775	26.481	26.606	26.621	0.148
50	1.37898	1.38153	1.37538	37.926	37.996	37.827	37.916	0.085
60	1.69215	1.72152	1.71311	46.539	47.347	47.115	47.000	0.416
120	2.15498	2.14352	2.15052	59.268	58.953	59.145	59.122	0.159
180	2.24318	2.24114	2.21015	61.694	61.637	60.785	61.372	0.509
240	2.41521	2.43154	2.41736	66.425	66.874	66.484	66.594	0.244
300	2.53216	2.54021	2.53542	69.641	69.863	69.731	69.745	0.111
360	2.60131	2.60435	2.59643	71.543	71.627	71.409	71.526	0.110
420	2.68318	2.69010	2.67643	73.795	73.985	73.609	73.796	0.188
480	2.71738	2.71539	2.71199	74.735	74.681	74.587	74.668	0.075
540	2.79314	2.79153	2.79544	76.819	76.775	76.882	76.825	0.054
600	2.82434	2.83012	2.82740	77.677	77.836	77.761	77.758	0.080
1440	2.89313	2.89194	2.89013	79.569	79.536	79.487	79.531	0.042

Solution of encapsulation and drug loading efficiency

1 mg/ mL of SA-GA-TMC in 1 mL of DI water for determined the encapsulation of simvastatin loaded the SA-GA-TMC micelles was absorbed at 12.152 ppm.

From
$$EE\% = \left(\frac{\text{amount of drug loaded in the micelles}}{\text{amount of drug added during fabrication}} \right) \times 100\%$$

Changes a unit from ppm to mg

$$1000 \text{ mL with } 12.152 \text{ mg}$$

$$\text{If } 1 \text{ mL with } (12.152 \times 1) / 1000$$

It was diluted to 3 times, so $((12.152 \times 1) / 1000) \times 3 = 0.03964 \text{ mg}$

From mass 55 mg of 10% SV/SA-GA-TMC has the drug 5 mg

$$\text{If } 1 \text{ mg equal to } (5 \times 1) / 55 = 0.091 \text{ mg}$$

So the encapsulation of SA-GA-TMC within 10% SV = $(0.039 / 0.09) = 44.44\%$

From

$$DL\% = \left(\frac{\text{amount of drug loaded in the micelles}}{\text{the total amount of drug in the micelles and SA-GA-TMC used in the process}} \right) \times 100\%$$

So $(0.039 / 1) \times 100 = 3.90\%$



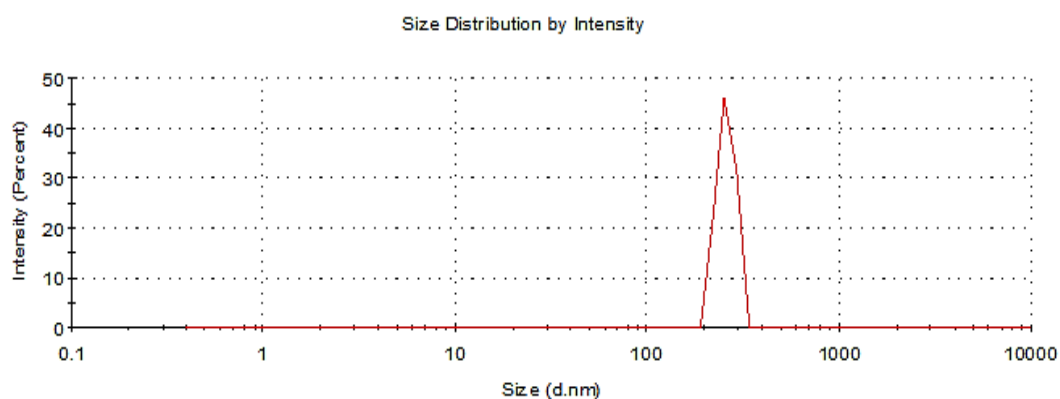


Figure 1D Particle size of SA-GA-TMC micelles without SV.

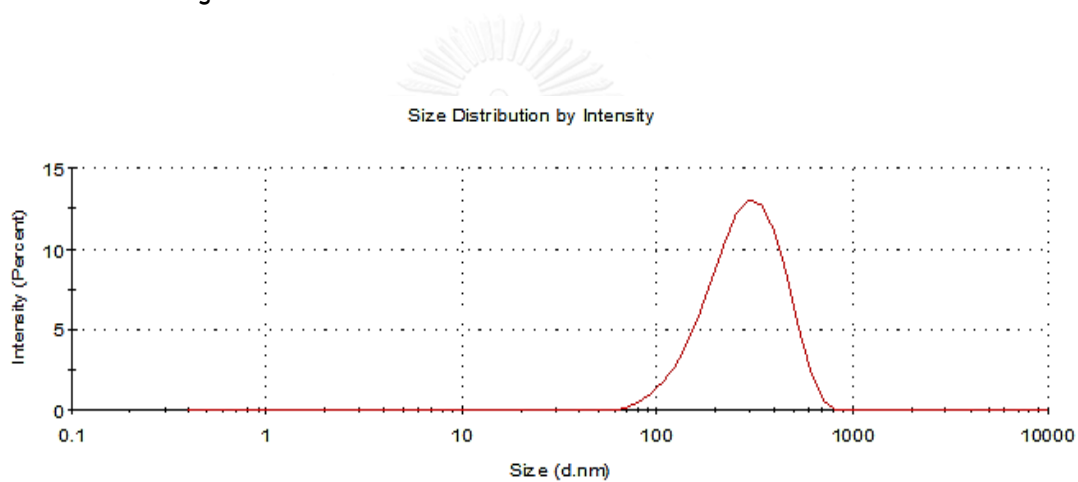


Figure 2D Particle size of SA-GA-TMC micelles with 10% SV.

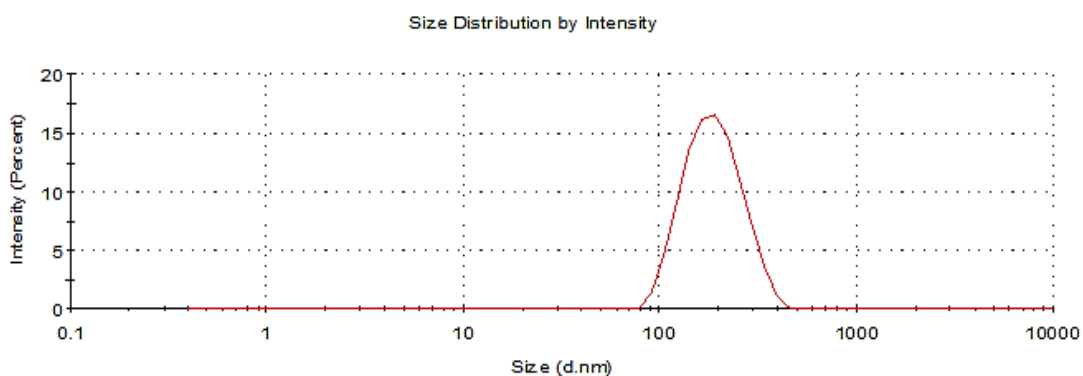


Figure 3D Particle size of SA-GA-TMC micelles with 20% SV.

VITA

Jakkri Nunthaviriyant was born on March 24, 1990 in Nonthaburi, Thailand. He received Bachelor Degree of Engineering in Petrochemical and Polymeric Materials from Silapakorn University in 2012. Since 2013, he has become a student in Master degree of Chulalongkorn University studying in Program of Petrochemical and Polymer since, Faculty of Science, Chulalongkorn University.

